

# Fylla Bank: structure and evolution of a normal-to-shear rifted margin in the northern Labrador Sea

Arne Døssing<sup>1,2</sup>

<sup>1</sup>DTU Space, National Space Institute, DK-2100 Copenhagen, Denmark. E-mail: ards@space.dtu.dk

<sup>2</sup>Institute of Geography and Geology, University of Copenhagen, Øster Voldgade 10, DK-1350 Copenhagen, Denmark

Accepted 2011 August 4. Received 2011 August 3; in original form 2011 February 5

## SUMMARY

Cenozoic seafloor spreading between Greenland and North America is generally considered a major right-stepping ridge-transform-ridge system between NW–SE trending spreading ridge segments in the Labrador Sea and Baffin Bay. The ridges were linked by N–S/NNE–SSW trending transform motions in the Davis Strait, in particular expressed by the ~1000-km-long Ungava Fault Zone. Fylla Bank, part of the southern West Greenland continental margin, is located in the northernmost Labrador Sea at the transition between the normal and shear rifting regimes of the Labrador Sea and Davis Strait. As such, the Bank may be compared with the Demerara Plateau, part of the French Guinea–Northeast Brazil continental margin. Seismic reflection interpretations presented in this study show that Fylla Bank is situated above an extensive basin complex, herein referred to as Fylla Structural Complex, which contains an up to 5-km-thick Cretaceous–Cenozoic sedimentary succession above an inferred pre-Cretaceous basement. Seismic mapping of basement structures show that the complex is dominated by NNW–NW-striking rift basins in its southern part and NNE-striking rift basins in its northern part. The rift basins are interpreted to be the result of an initial late-Early Cretaceous rift phase, which mainly resulted in the formation of the NNW–NW-striking structures, and a subsequent early Campanian rift phase, mainly resulting in the formation of large NNE-striking rotated fault blocks. Resumed rifting in the early Cenozoic deepened the NNE-striking rift basins. The NNE-oriented structures have previously been interpreted to initiate during the latest Cretaceous. However, this study suggests that they initiated transfer faults already during the late-Early Cretaceous rift phase and possibly correlate with along-strike discontinuities in oceanic crust in the Labrador Sea to define margin segmentation in southern West Greenland, including the borders of Fylla Bank. A structural-kinematic model presented here thus suggests that the Cretaceous–Cenozoic poly-phase rifting to some extent was controlled by pre-existing crustal fabric. Combined with an interpreted interplay between normal stresses in the Labrador Sea and oblique-shear stresses in the Davis Strait, this resulted in a very complex structural-tectonic evolution and the formation of several distinct structural styles. The seismic interpretations are supported by maps of the Moho topography and crustal thickness which were compiled from results of pseudo-3-D gravity modelling. The maps show minimum crustal thicknesses (11 km) and maximum Moho uplifts in areas where the NNW–NW- and NNE-striking structures interact. Moreover, a strong correlation is found between Moho topography, crustal attenuation, rift-enforced thermal uplift and erosion, and post-rift subsidence in the area. This is interpreted to be a result of thermally controlled basin dynamics.

**Key words:** Continental margins: divergent; Continental margins: transform; Continental tectonics: extensional; Crustal structure; Arctic region.

## 1 INTRODUCTION

Studies of passive continental margins have demonstrated a great variety in crustal structures depending on the style of deformation during the intracontinental rifting phase—the two end-members being normal rifted and transform margins. While rifted margins

often display a wide Ocean–Continental–Transition (OCT) zone that is characterized by large rotated fault blocks and infilled by syn-kinematic sediments (Mjelde *et al.* 2005), transform margins are generally characterized by a very narrow OCT, marginal basement highs and absence of upper crustal fault blocks (e.g. Keen *et al.* 1990a; Basile *et al.* 1998; Døssing *et al.* 2008). Recent studies

of intermediate-style, oblique-shear margins (Faleide *et al.* 1993; Wilson *et al.* 2003; Greenroyd *et al.* 2008; Døssing *et al.* 2010a) have demonstrated structural segmentation of the margins by transform faults that divide the margins into rift- and transform-style structures. This highlights the effect of transtensional stresses at margins lying oblique to the mid-ocean ridge, where the transform faults can often be correlated with along-strike discontinuities at the mid-ocean ridge.

The Labrador Sea is confined between the coasts of Labrador, SE Baffin Island and southern West Greenland (Fig. 1). To the southeast, the sea is more than 3500 m deep and 900 km wide and

opens into the Atlantic Ocean. To the north, it narrows and passes into the 300 km wide Davis Strait, a shallow seaway leading into the deeper Baffin Bay farther north. The margins of the Labrador Sea and the Davis Strait are characterized by complexes of large Mesozoic–Cenozoic sedimentary basins that were initiated by rifting during Early Cretaceous time. This eventually led to opening of the Labrador Sea along an early NW-propagating branch of the Mid-Atlantic Ridge (e.g. Srivastava 1978; Chalmers & Pulvertaft 2001) and development of conjugate, normal rifted margins off southern West Greenland and Labrador and a transform margin in the Davis Strait (e.g. Srivastava 1978; Srivastava & Tapscott 1986; Chalmers

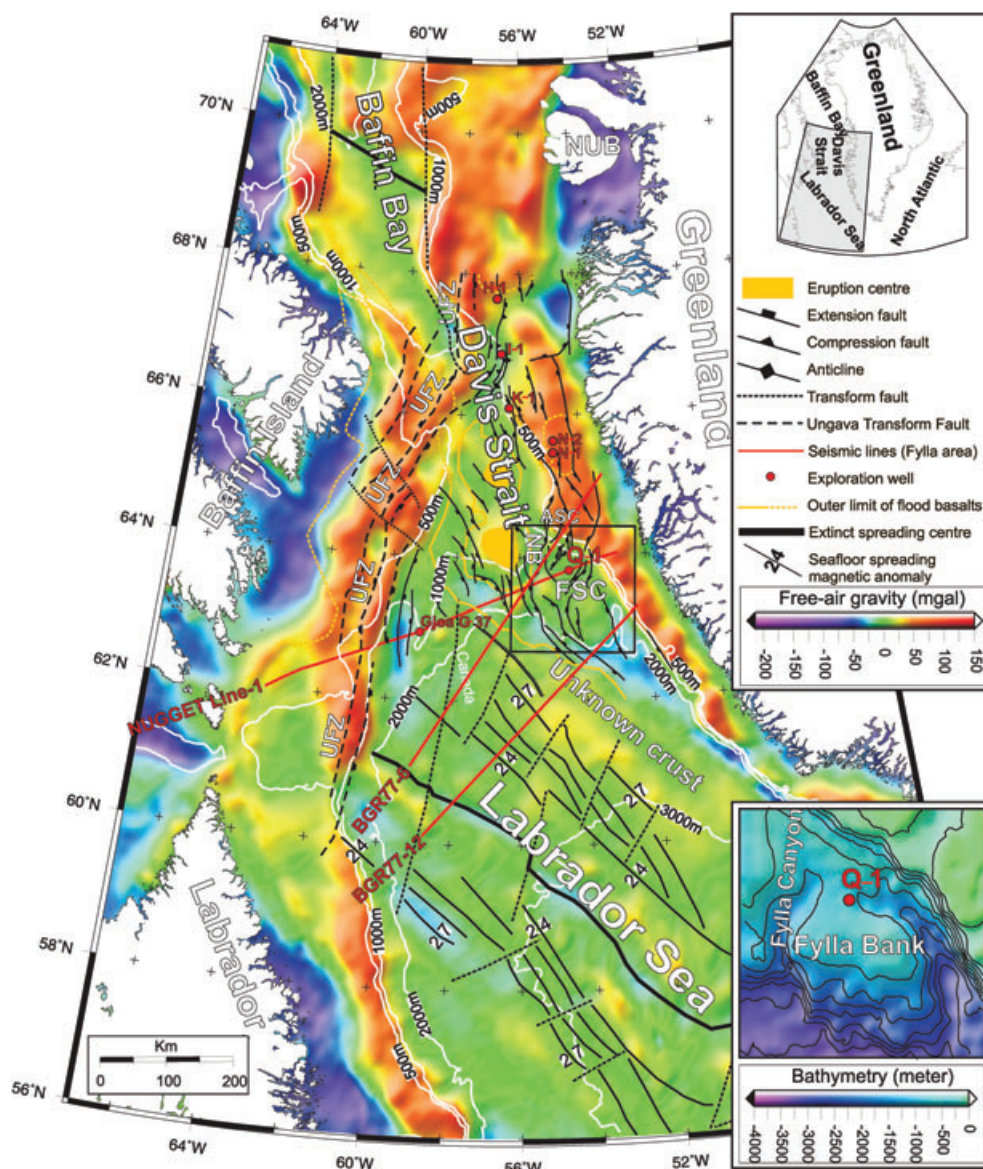


**Figure 1.** Map of Free-air gravity anomalies of the Labrador Sea, Davis Strait and Baffin Bay. Bathymetric contours (500 m, 1000 m and 2000 m) and main tectonic features are shown on the map. Note that the map only shows the extent of agreed oceanic crust (Chron 27N and younger) in the Labrador Sea. ‘Unknown crust’ refers to the zone between anomaly 27 and the shelf break, where oceanic crust (Chron 33–27) has been interpreted by, for example, Srivastava (1978) and Roest & Srivastava (1989a), while thin and foundered continental crust has been interpreted by, for example, Chian & Loudon (1994) and Chalmers & Pulvertaft (2001). The black box shows location of Fylla Bank. Note the relatively small free-air gravity anomalies over the Bank indicating that it is compensated at depth. Lower inset figure: Bathymetry of Fylla Bank. The outline of the area corresponds to the black box in the main figure. H-1 (Hellefisk-1), I-1 (Ikermiut-1), K-1 (Kangamiut-1), N-1 (Nukik-1), N-2 (Nukik-2) and Q-1 (Qulleq-1) refer to released exploration wells on the West Greenland Shelf. None of the wells have penetrated the deepest seismic sequences (Rolle 1985). Other abbreviations used: ASC, Atammik Structural Complex; FSC, Fylla Structural Complex; NB, Nuuk Basin; NUB, Nuugssuaq Basin; UFZ, Ungava Fault Zone.

*et al.* 1993; Srivastava & Roest 1999; Chalmers & Pulvertaft 2001; Nielsen *et al.* 2002). This study focuses on Fylla Bank (Fig. 1, lower inset figure), which is located in the northernmost Labrador Sea at the transition between the normal rifted margins of southern West Greenland and the shear rifted margins of West Greenland in Davis Strait. The Bank is outlined by an ~1000-m-deep and 120–150-km-wide plateau between the deep Labrador Sea to the south-west and the less than 200-m-deep southern West Greenland Shelf to the northeast. Deep canyons bound the plateau to the west (Fylla Canyon) and east. Regional seismic studies of the southern West and West Greenland margins have demonstrated that Fylla Bank is seated on an extensive basin complex (Bate *et al.* 1994; Chalmers & Pulvertaft 2001; Funck *et al.* 2007), herein is referred to as Fylla Structural Complex (FSC). However, the interaction of normal-to-shear rifting in FSC has not been studied before. Given the broad range of available geological and geophysical data, this relatively confined basin complex therefore offers a unique opportunity to study the evolution of a normal-to-shear rifted continental margin.

This study presents the first detailed interpretation of the structural and tectonic evolution of FSC based on multichannel seismic (MCS) reflection data, borehole and gravity data as well as a recently published wide-angle/refraction seismic velocity profile (Funck *et al.* 2007). A complex structural and tectonic evolution is revealed and evidence is shown of Cretaceous–Cenozoic normal-to-shear poly-phase rifting that resulted in several distinct rift basins interacting in space and time. Evidence is also shown for structural control by NNE-striking transform faults, which are (sub) parallel to the major Ungava Fault Zone in the Davis Strait (Fig. 1) and to along-strike discontinuities in the oceanic crust in the Labrador Sea. The interpreted structural evolution is supported by analysis of syn- and post-rift basin kinematics in relation to crustal thickness and Moho topography; the latter compiled from 2-D and pseudo-3-D gravity modelling.

## 2 GEOLOGICAL SETTING

### 2.1 Plate kinematic evolution

Marine magnetic, gravity and seismic data indicate that the central Labrador Sea is underlain by oceanic crust to the south-east of the Ungava Fault Zone (Fig. 1, Srivastava 1978; Roest & Srivastava 1989a,b; Keen *et al.* 1990b; Chian *et al.* 1995a; Srivastava & Roest 1999; Chalmers & Pulvertaft 2001), while seismic refraction (Keen & Barrett 1972) and seismic reflection (Chalmers & Pulvertaft 2001) interpretations are consistent with extended continental crust in the Davis Strait. It is generally agreed that the Labrador Sea formed by seafloor spreading along an early NW-propagating branch of the Mid-Atlantic Ridge. This has caused the separation of Greenland from North America and the development of normal rifted continental margins off southern West Greenland and Labrador and a transform rifted margin off central West Greenland (Srivastava 1978; Chalmers *et al.* 1993; Srivastava & Roest 1999; Chalmers & Pulvertaft 2001; Nielsen *et al.* 2002). Dating of coast-parallel intrusives suggests that continental rifting between Greenland and Canada initiated in the Early Cretaceous (131–104 Ma, Umpleby 1979; 138–133 Ma, Larsen *et al.* 1999). At the beginning of Late Cretaceous rifting ceased in the northern part of the Labrador Sea and a global sea level rise combined with thermal subsidence resulted in regional marine conditions and deposition of post-rift sediments (Chalmers *et al.* 1993; Chalmers 1997; Chalmers & Pulvertaft 2001).

Continental break-up and seafloor spreading in the Labrador Sea is proposed to have begun during magnetochron 33 (79.7–74.5 Ma, early Campanian), causing a counter-clockwise rotation of Greenland relative to North America (Srivastava 1978; Roest & Srivastava 1989a,b; Srivastava & Roest 1995, 1999). This interpretation is based on the assumption that the continent–ocean boundary is located at the shelf break. However, other models suggest that true seafloor spreading (average stretching half rate  $>15 \text{ mm a}^{-1}$ ) did not begin before the early Palaeocene which is based on chron 27N (61 Ma) as the oldest positively identified spreading anomaly in the Labrador Sea (Chalmers 1991; Chalmers *et al.* 1993; Chalmers & Laursen 1995; Chian *et al.* 1995a). An ~100-km-wide crustal transition zone, consisting of thin and foundered continental crust, is suggested to exist between the shelf break and anomaly 27N (e.g. Chian & Loudon 1994; Chian *et al.* 1995a,b; Loudon & Chian 1999).

Large areas were affected by flood basalt volcanism along the margins of SE Baffin Island and West Greenland during chron 27N (~60.9–61.3 Ma, early Palaeocene) possibly related to impact of the Icelandic mantle plume west of Greenland. Basaltic volcanic activity resumed during chron 24R (55.9–53.3 Ma, early Eocene) coinciding with a change in relative spreading direction from initially ENE–WSW to NE–SW and opening of the North Atlantic (Srivastava 1978; Srivastava & Roest 1995, 1999; Storey *et al.* 1998; Chalmers & Pulvertaft 2001; Riisager *et al.* 2003). Seafloor spreading in the Labrador Sea slowed down around chron 20 (35 Ma, latest Eocene) and died out entirely by chron 13 (33 Ma, earliest Oligocene), leaving an extinct NW–SE trending spreading centre in the central Labrador Sea (e.g. Srivastava 1978; Srivastava & Roest 1995, 1999; Chalmers & Pulvertaft 2001).

### 2.2 The West Greenland Basin

The southern and central West Greenland margins are characterized by a complex of large sedimentary basins (Fig. 1) unconformable overlying an inferred Top pre-Cretaceous basement surface (e.g. Chalmers & Pulvertaft 2001; Sørensen 2006). The basins consist of disconnected wedges of Lower Cretaceous basalts, pre- and syn-rift sediments, which are unconformable overlain by Upper Cretaceous and younger strata, generally assigned to the post-rift terrace wedge (Fig. 2). The West Greenland Basin extending from 63°N to 68°N is thoroughly described in, for example, Chalmers *et al.* (1993), Chalmers & Pulvertaft (2001), Dalhoff *et al.* (2003a) and Sørensen (2006). FSC constitutes the south easternmost part of the West Greenland Basin and is bordered by the Atammik Structural Complex to the north and the Nuuk Basin (NB) to the west (Fig. 1). To the southeast, the continental shelf narrows, the basins becomes smaller and the continental slope turns into a major fault scarp (Chalmers *et al.* 1993; Chalmers 1997; Chalmers & Pulvertaft 2001). The earliest regional seismic studies near FSC (Fig. 1: Lines BGR77–6 and –12) revealed the presence of rotated fault blocks (Chalmers 1991; Chalmers & Laursen 1995), and later it was suggested that the Complex is dominated by NW/NNW-striking faults of presumed Early Cretaceous age and major NNE-striking fault blocks (Bate *et al.* 1994; Isaacson & Neff 1999) of presumed Palaeogene age (Chalmers & Pulvertaft 2001). Seismic refraction studies further indicate that the continental crust is only ~14 km thick beneath the central part of FSC but more than 18–20 km thick beneath the inner southern West Greenland Shelf and beneath the SW-edge of FSC towards the Labrador Sea (Funck *et al.* 2007).

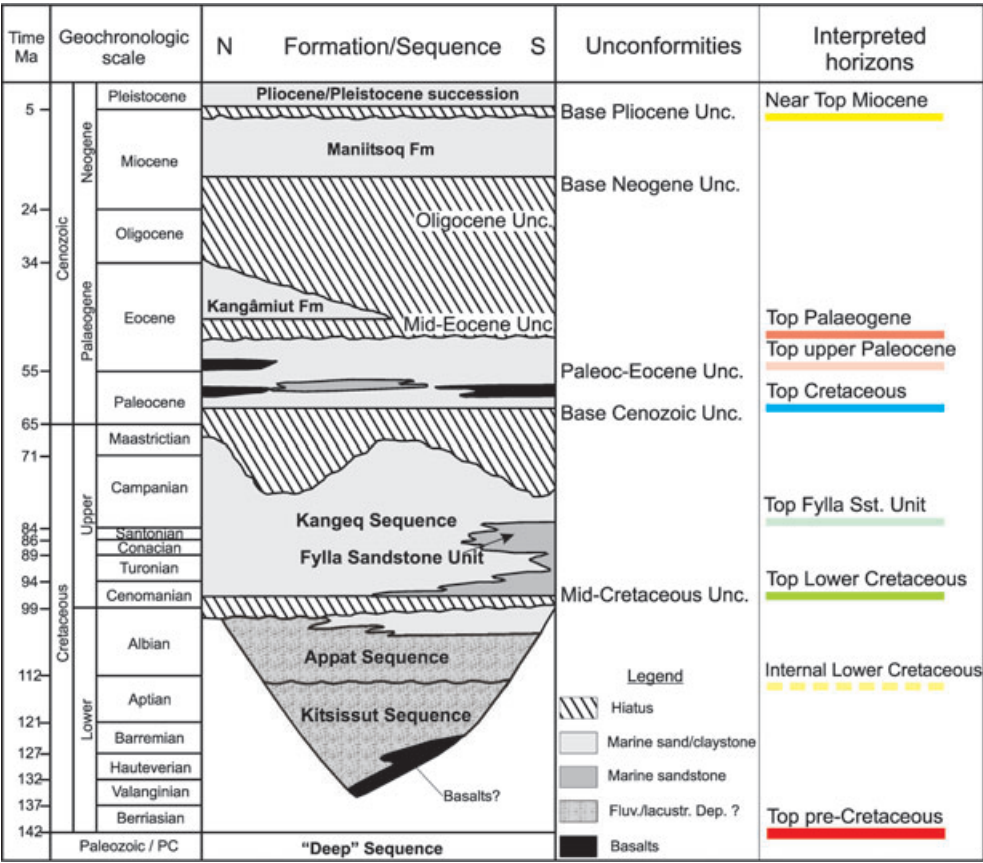


**Figure 2.** Generalized stratigraphy for the southern West Greenland Shelf. Modified from Chalmers & Pulvertaft (2001) and Sørensen (2006). Note that the major mid-Eocene and Oligocene Unconformities merge to a significant Base Neogene Unconformity in the Fylla area (Dalhoff *et al.* 2003a; Nøhr-Hansen 2003). The seismic horizons interpreted in this study are shown in the right column.

3 SEISMIC REFLECTION INTERPRETATION

3.1 Data

This study is mainly based on MCS reflection data acquired from 1977 to 1999 by TGS-NOPEC, Bundesanstalt für Geowissenschaften und Rohstoffe (BGR), Nunaolil, Statoil and the Geological Survey of Greenland (GGU); the latter now part of the Geological Survey of Denmark and Greenland (GEUS). The MCS data constitute an overall NW–SE/NE–SW-oriented rectangular grid that covers Fylla Bank; an area of approximately 15 000 km<sup>2</sup> (Fig. 3). The seismic profiles were used to subdivide the sediments by seven horizons on the basis of their internal reflective character and upper and lower reflector terminations (Fig. 2): (1) Top pre-Cretaceous; (2) Top Lower Cretaceous; (3) Top Fylla Sandstone Unit; (4) Top Cretaceous; (5) Top upper Palaeocene; (6) Top Palaeogene (Top lower Eocene) and (7) Near Top Miocene. The Qulleq-1 (Q-1) exploration well was drilled into the crest of a rotated fault block in the central part of FSC in the year 2000. Depth-to-time converted data from this borehole were used for dating the interpreted seismic sequences. However, the borehole only penetrates Upper Cretaceous sediments, that is, only the upper part of the visible seismic sequences (Fig. 4). Dating of the deepest seismic sequences is in the following based on correlation with analogue seismic sequences drilled on the Labrador Shelf.

3.2 Seismic stratigraphy

3.2.1 Top pre-Cretaceous basement

The acoustic and structural basement in FSC is generally defined by a fairly continuous and high-amplitude reflection (Figs 4 and 5), which is interpreted as the Top pre-Cretaceous unconformity. A seismic cross-section (see Supplementary Information, Fig. S1) shows evidence of truncated and folded sediments beneath the Top pre-Cretaceous surface, possibly reflecting Lower Palaeozoic carbonate rocks, which have been found in a grab sample from the bottom of Fylla Canyon (see Fig. 3 for location) (*cf.* Dalhoff *et al.* 2003b). Similar interpretation has also been proposed elsewhere in the Labrador region (e.g. Bell & Howie 1990; Balkwill *et al.* 1990; Sørensen 2006).

3.2.2 Lower Cretaceous succession

Sediments above the basement can be divided into two successions separated by a regional unconformity surface of presumed mid-Cretaceous age (the Mid-Cretaceous Unconformity, Figs 2, 4 and 5). The lower, fault-bounded succession unconformable overlies the basement in basinal parts of the area (Fig. 5). This succession can be divided into a lower, dominantly pre-rift sequence characterized by fairly even and subparallel reflections of low-to-medium amplitude and an upper syn-rift sequence characterized by medium-amplitude

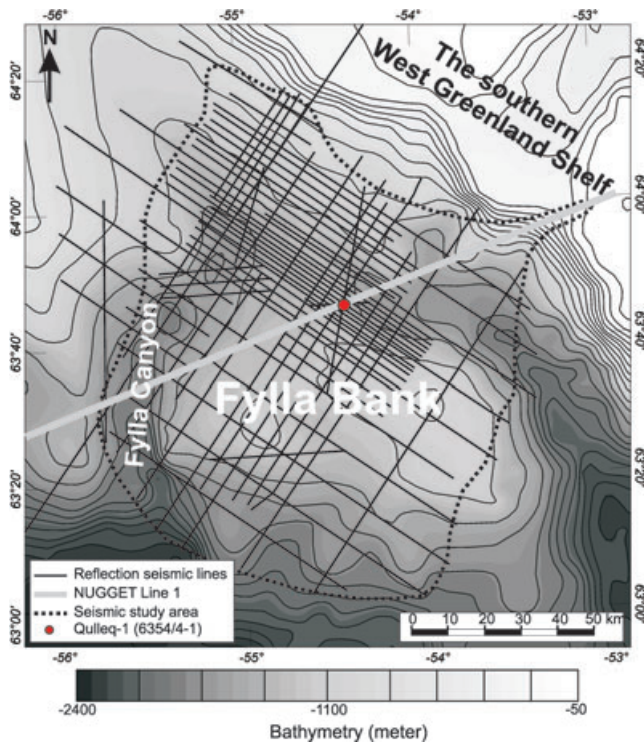


**Figure 3.** Seismic lines interpreted in this study. The MCS reflection lines include the entire Nuna9401 and ST9708 surveys as well as selected lines from the ST9902 survey (line ST9902–01001), the VEST SEIS 1992 survey (lines GGU1/92–22 and GGU1/92–22A) and the BRG-1977 survey (line BGR1/77–6). In total, 61 lines constituting more than 8000 km have been interpreted. Also shown are the location of the deep exploration well Q-1 (Quilleq-1, 6354/4-1) and the wide-angle/refraction seismic NUGGET Line 1. Background shows bathymetry of Fylla Bank. Note the deep canyons that border the Bank to the west (Fylla Canyon) and east. Projection: UTM Zone 21 (Central meridian 57°W).

reflections that show strong divergence towards the bounding faults. The two sequences are here referred to as the Kitsissut and Apat Sequences based on their strong seismic resemblance with the Lower and Upper Members of the Bjarni Formation on the conjugate Labrador Shelf (Fig. 5, inset figure). These are of Barremian–Aptian (mid-Early Cretaceous) and Aptian–Albian age (late-Early Cretaceous), respectively (Balkwill *et al.* 1990; Chalmers & Pulvertaft 2001) and have been used as analogues for the pre- and syn-rift Kitsissut and Apat Sequences interpreted elsewhere on the West Greenland Shelf (Chalmers *et al.* 1993; Chalmers & Pulvertaft 2001; Sørensen 2006).

### 3.2.3 Upper Cretaceous succession

The Lower Cretaceous succession is throughout FSC unconformably overlain by the Fylla Sandstone Unit, which shows progressive onlap over the lower parts of basement structural highs (Fig. 5). This unit is generally defined by a relatively transparent lower interval and a highly reflective upper interval of continuous reflections. The upper interval constitutes the deepest penetrated sediments in Q-1 and comprises a fully marine sandstone succession of Late Santonian age (Fig. 4). The overlying Kangeq Sequence exhibits a fairly homogeneous character throughout the study area with well-stratified and low-to-medium amplitude continuous reflections (Figs 4 and 5). In Q-1, the Sequence comprises a fully marine mudstone of early Campanian age. Although indicated by

the seismic interpretations, there are no signs of an unconformity or a condensed section at the boundary between the Fylla Sandstone Unit and the Kangeq Sequence in Q-1. Also, no erosional unconformities have been observed within the Kangeq Sequence (*cf.* Nøhr-Hansen *et al.* 2000; Christiansen *et al.* 2001).

### 3.2.4 Base Cenozoic unconformity

The Upper Cretaceous succession in FSC is terminated by the diachronous and erosive boundary of the Base Cenozoic Unconformity, which is defined by angular truncation of the underlying reflections and a general onlap over structural highs of the overlying reflections (Fig. 4).

### 3.2.5 Cenozoic succession

The seismic interpretations show that the Cenozoic succession exhibits a well-stratified, Palaeocene to Quaternary mudstone dominated and deep marine succession, which contains several unconformities (Fig. 4). The unconformities, traceable offshore southern West Greenland in general (see Fig. 2), have been related to series of uplift events (Rolle 1985; Chalmers 2000; Japsen *et al.* 2006).

## 4 STRUCTURE AND EVOLUTION OF FSC

In the following, the structural configuration of FSC (Fig. 6) and its (mainly Cretaceous) evolution are presented based on the mapped seismic horizons. The interpretations are illustrated by representative seismic profiles (Figs 4, 5 and 7–10) and summarized by seismic isochore maps (Fig. 11). Abbreviations are explained in Table 1.

### 4.1 Basement structures

The mapped Top pre-Cretaceous basement (Fig. 6) reveals a setting of NW–NNW- and NNE-striking intersecting rift basins that form a separation of three basement highs, here termed the Fylla West High (FWH), Fylla North High (FNH) and Fylla East High (FEH). The highs are characterized by being relatively non-faulted and overlain by sediments of Late Cretaceous age and younger (*cf.* Fig. 10a).

The NW–NNW-striking rift basins, Fylla East Basin (FEB), Fylla Central Basin (FCB) and Paamiut Basin (PB), display significantly contrasting structural styles. The NNW-striking FEB to the east and north is defined by high-angle faults that downthrow basement to the northeast forming a series of downstepping half-grabens of which the largest is more than 10 km wide in cross-section (Figs 5 and 10b). In contrast, the central part of FSC is dominated by the NW-striking FCB, which is roughly 60 km long, 25 km wide and defined by SW-dipping faults that detach in a major low-angle SW-dipping detachment plane (Figs 6 and 7). Finally, the NNW–NW-striking PB to the south is characterized by a major half-graben bounded by a steep SW-dipping fault (Fig. 10c). A similar half-graben is located to the northwest of FCB (Fig. 6, ‘PB related structure’).

The NNE-striking rift basins, Fylla Fault System-1 (FFS-1) and -2 (FFS-2), dominate the northern part of FSC (Fig. 6). The major FFS-1 is composed of six rotated fault blocks that are bounded by ESE-dipping faults (Fig. 8). Some of the faults of FFS-1 continue to the south where they offset the NNW–NW-striking faults of FEB and FCB (Fig. 6, ‘triple junction area’). To the northwest of FFS-1, FFS-2 constitutes a narrow zone of subparallel and anastomosing faults that intersect FNH (Fig. 6). The main part of FFS-2 comprises

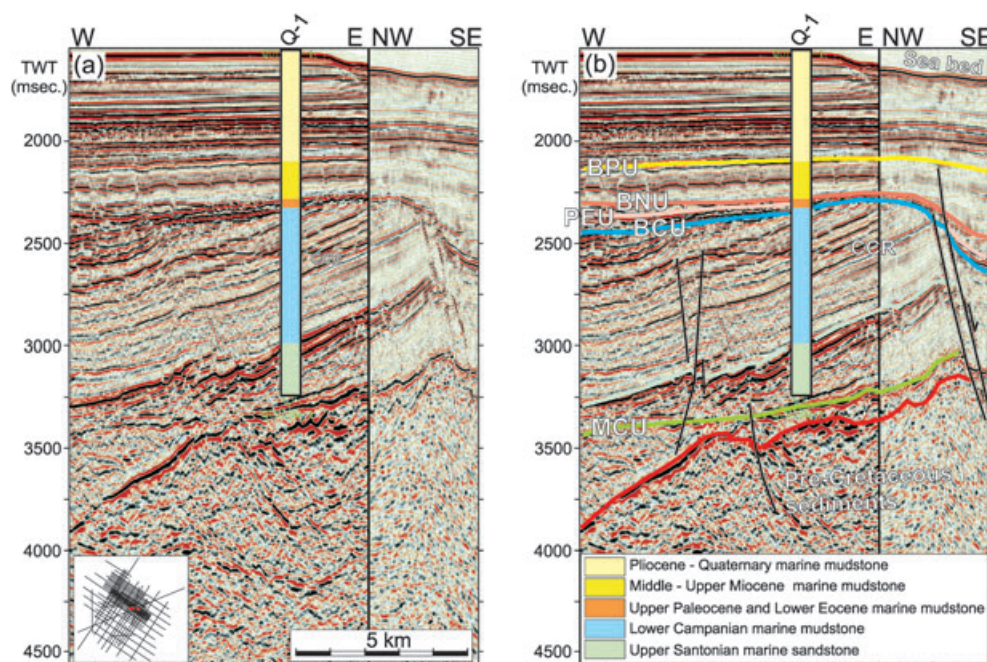


**Figure 4.** Borehole-to-seismic tie for Q-1. (a) Uninterpreted time migrated MCS profile and (b) interpreted profile. See Fig. 2 for colour coding of the interpreted seismic horizons. The depth-to-time converted borehole stratigraphy is based on Christiansen *et al.* (2001). Note the major Base Neogene Unconformity which separates thick, well-stratified Miocene and Plio-Pleistocene sediments above from a thin succession of contorted, high-amplitude reflections of Upper Palaeocene–Lower Eocene sediments beneath. Note also the angular Base Cenozoic Unconformity, which separates tilted and truncated lower Campanian sediments of the Kangeq Sequence from Upper Palaeocene sediments (Nøhr-Hansen *et al.* 2000; Christiansen *et al.* 2001; Pegrum *et al.* 2001; Dalhoff *et al.* 2002); a hiatus interval of *ca.* 20 Ma possibly relating to an early Palaeocene uplift and erosion caused by the impact of the Icelandic plume (*cf.* Section 2.1). Finally, note that the borehole does not penetrate the deepest visible sediments above the interpreted Top pre-Cretaceous basement. Abbreviations: BCU, Base Cenozoic Unconformity; BNU, Base Neogene Unconformity; BPU, Base Pliocene Unconformity; MCU, Mid-Cretaceous Unconformity; PPU, Palaeocene-Eocene Unconformity; CCR: Cross-Cutting Reflection.

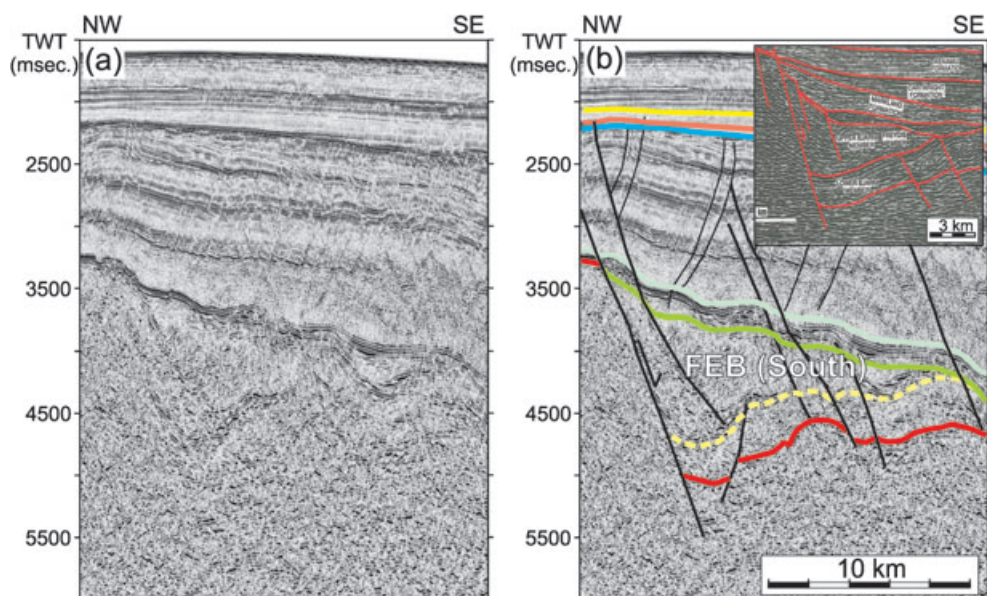


**Figure 5.** Time migrated MCS profile across the southern part of the NNW-striking Fylla East Basin (FEB). (a) Uninterpreted profile and (b) interpreted profile. See Fig. 6 for location. See Fig. 2 for colour coding of the interpreted seismic horizons. The seismic profile shows a large half-graben infilled with the Lower Cretaceous pre- and syn-rift Kitsissut and Appat Sequences. The Sequences are separated from Upper Cretaceous sediments of the Fylla Sst. Unit and Kangeq Sequence by the erosional Mid-Cretaceous Unconformity. Upper right inset figure shows an interpreted seismic cross-section from the Labrador Shelf (Balkwill *et al.* 1990) of a similar half-graben infilled with the pre- and syn-rift Lower and Upper Members of the Bjarni Formation. These are of Barremian–Aptian (mid-Early Cretaceous) and Aptian–Albian age (late-Early Cretaceous). Note the strong seismic resemblance with the interpreted Kitsissut and Appat Sequences in FEB.

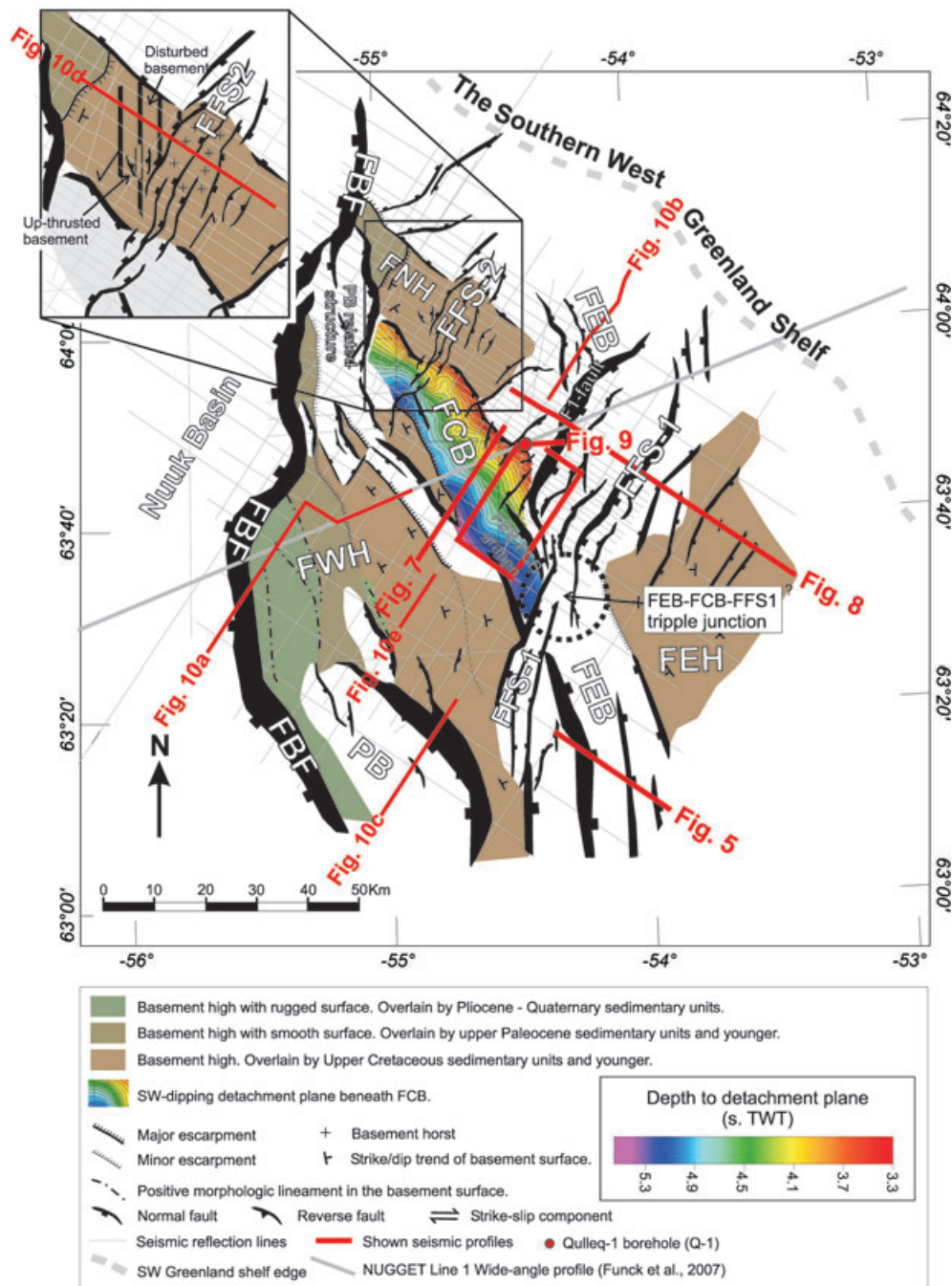


**Figure 6.** Map of Top pre-Cretaceous basement structures in FSC interpreted from MCS reflection data in this study. See Table 1 for abbreviations used. The coloured lines show locations of presented seismic profiles. Note that the southern part of FSC in general is dominated by NNW-/NW-striking structures (PB, FEB, FCB and FBF as well as NW-/NNW-striking basement lineaments over the southwestern most part of FWH), while the northern part of the Complex is dominated by NNE-striking structures (FFS-1, FFS-2 and FBF). The NW-, NNW- and NNE-striking structures overlap in the ‘triple junction area’. Note also that the NNW-striking FEB is interpreted both in the eastern and northern part of the study area and that it appears to be offset in a right-lateral direction along FFS-1.

two, approximately 20-km-long and 4-km-wide, shallow basement horst blocks which are bounded by nearly vertical faults (Fig. 10d). A few faults extend farther south where they define a number of small fault blocks that offset the NW-striking FCB (Fig. 6).

The dominating NNW-, NW- and NNE-orientations within FSC are also mapped along the FBF that defines the border between FSC and the deep NB to the west/southwest (Fig. 6). The FBF shows an overall N–S orientation but is composed by individual

fault segments with distinct NNW-, NW- and NNE-orientations, hence suggesting a close relationship with the interpreted structures in FSC.

#### 4.2 Late-Early Cretaceous rifting

The NNW-/NW-striking rift basins (FEB, FCB and PB) are infilled with pre- and syn-rift sediments of the Kitsissut and Appat

Sequences indicating that significant rifting took place in FSC during the late-Early Cretaceous (Fig. 11a). Pronounced extension across the NNW/NW-striking structures is, for example, indicated by the major basement block in FCB (see Fig. 7) that appears to have rotated and glided approximately 10 km along the detachment plane to the southwest. Note that fault-bounded Lower Cretaceous sediments are also interpreted within the deeper parts of the NNE-striking FFS-1 (Figs 8 and 11a) suggesting that late-Early Cretaceous rifting affected this structure as well. This is supported by the interpretation of the NNW-striking FEB to the south and north of FFS-1 (see Fig. 6), that is, the NNE-striking FFS-1 faults may have initiated transtensional transfer faults during late-Early Cretaceous rifting (*cf.* Section 6.3). Late-Early Cretaceous rifting most likely affected FBF (Figs 10a and 11a), where pre- and syn-rift units similar to the Kitsissut and Appat Sequences in FSC constitute the deepest visible sedimentary infill in the NB. The NB is not the primary issue of this paper and will not be treated further.

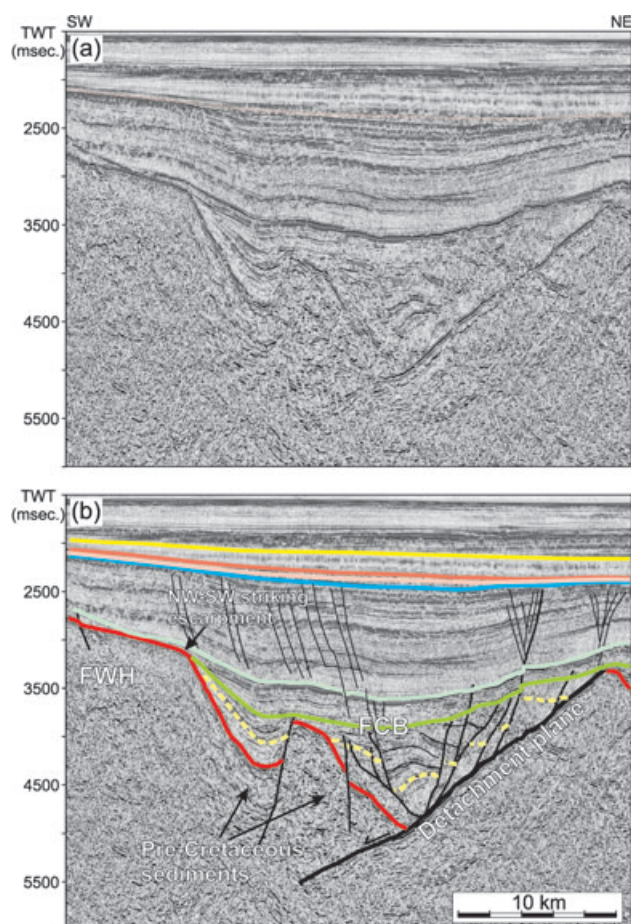


**Figure 7.** Time migrated MCS profile across the NW-striking Fylla Central Basin (FCB). (a) Uninterpreted profile and (b) interpreted profile. See Fig. 6 for location. See Fig. 2 for colour coding of the interpreted seismic horizons. The seismic profile shows the central part of FCB consisting of two half-grabens that are separated by a major basement block. The block appears to have rotated and glided ~10 km to the southwest along a major SW-dipping detachment plane that underlies the entire FCB (see Fig. 6). Farther to the northwest, FCB splits into three half-grabens while to the southeast the SW-dipping faults of FCB intersect with the NE-dipping faults of FEB, creating a deep graben (see Fig. 6 for location). The sedimentary units infilling FCB are truncated against the Mid-Cretaceous Unconformity and therefore interpreted to correlate with the Lower Cretaceous pre- and syn-rift Kitsissut and Appat Sequences of FEB (see Fig. 5).

The widespread distribution of Lower Cretaceous syn-rift sediments in FSC (Fig. 11a) and the formation (or reactivation) of several distinct structural styles with different orientations are interpreted to reflect a major late-Early Cretaceous rift phase where pre-existing structural weaknesses and local stress conditions possibly controlled the outcome of the rifting (*cf.* Section 6.3). Alternatively, the structural differences reflect two or more phases of Early Cretaceous rifting which, however, are not resolvable from the available data.

### 4.3 Mid-Cretaceous uplift and erosion

Following late-Early Cretaceous rifting, thermal uplift affected the Lower Cretaceous rift basins. This caused erosion of the Lower Cretaceous pre- and syn-rift sediments and exposure of pre-Cretaceous basement over shallow footwall blocks and basement highs as indicated by the widespread top angular truncation against the Mid-Cretaceous Unconformity (Figs 5, 7 and 10b and c). In the deep graben, which formed between the overlapping FEB and FCB (Fig. 6: FEB-FCB graben), the amount of Lower Cretaceous pre- and syn-rift sediments left (up to 0.5 s TWT) is less compared with the amount in the adjacent half-grabens of FCB (up to 0.8 s TWT) and FEB (up to 1.5 s TWT, Fig. 11a). This is interpreted as evidence of strong thermal uplift and erosion as response to significant crustal thinning (*cf.* Section 6.1).

### 4.4 Late Cretaceous post-rift subsidence

The truncated Lower Cretaceous rift basins are throughout the area draped by the marine upper Santonian Fylla Sandstone Unit and lower Campanian Kangeq Sequence (e.g. Figs 5 and 7). Both units were drilled in Q-1 (Fig. 4). The Upper Cretaceous units show non-fault-related thickening over FEB and FCB with distinct basal onlap towards and over the surrounding basement highs (Fig. 7). This indicates that thermally induced post-rift subsidence followed thermal uplift and erosion at the Mid-Cretaceous Unconformity. The upper Santonian Fylla Sandstone Unit represents the earliest post-rift unit and the development of a mixed deltaic and shoreface environment with deposition mainly being confined to narrow depocentres over the subsiding post-rift basins (Fig. 11b) and development of prograding deltas over the surrounding basement highs (Figs 10e and 11b). The shallowest parts of the highs probably remained sub-aerially exposed during this early post-rift phase. The subsequent deposition of thick piles of marine shales (up to 2 s TWT) of the Kangeq Sequence during the early Campanian (Fig. 11c) indicates a change to a relatively deep marine environment. This was likely forced by a combination of continued post-rift subsidence and rising eustatic sea levels (*cf.* Section 2.1). Deposition was still centred over the Lower Cretaceous rift basins (Figs 7 and 11c) but pronounced angular truncation of the Kangeq Sequence against the Base Cenozoic Unconformity over the shallowest parts the basement highs (Figs 7, 10a and 11c) indicates that the entire FSC was drowned during the early Campanian.

### 4.5 Lower Campanian rifting

The upper Santonian Fylla Sandstone Unit and lower Campanian Kangeq Sequence constitute the main sedimentary infilling of the NNE-striking FFS-1 and -2 with a maximum total thickness of almost 2 s TWT within the major FFS-1 rotated fault blocks (Figs 8, 11b and c). In Fig. 9, it is shown that important fault block rotation

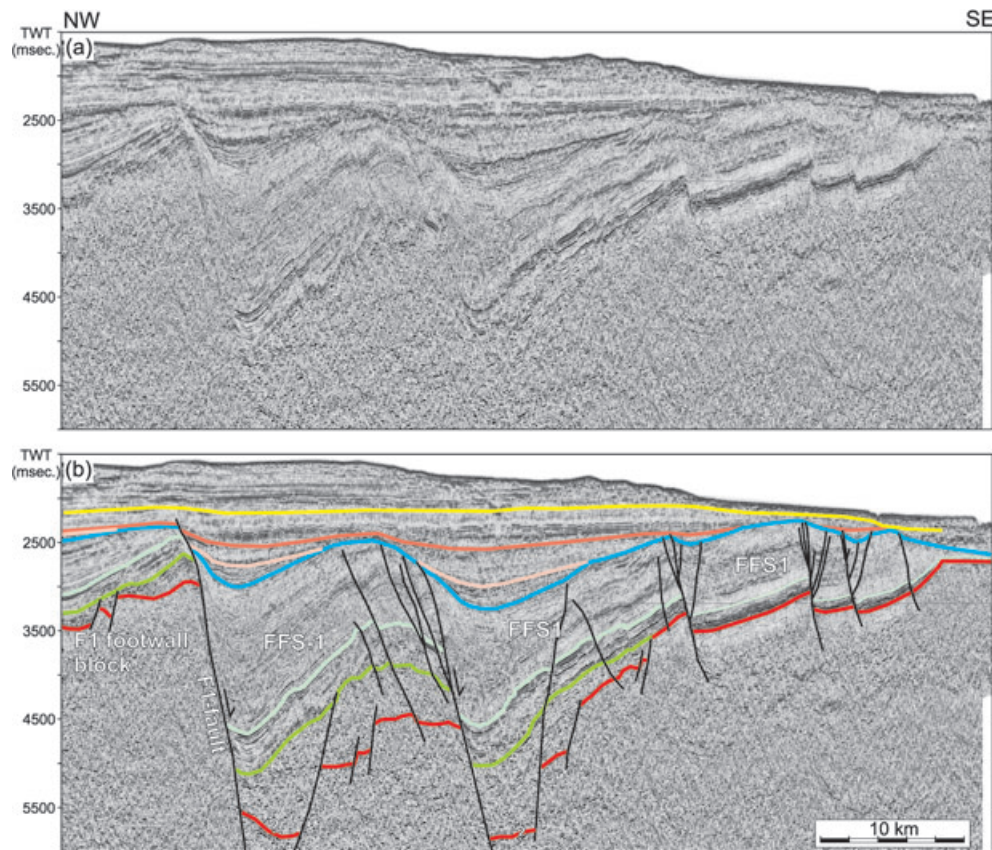


**Figure 8.** Time migrated MCS profile across the major rotated fault blocks of the NNE-striking Fylla Fault System-1 (FFS-1). (a) Uninterpreted profile and (b) interpreted profile. See Fig. 6 for location. See Fig. 2 for colour coding of the interpreted seismic horizons. The upper Santonian Fylla Sandstone Unit and lower Campanian Kangeq Sequence constitute the main sedimentary infilling of FFS-1 with a maximum total thickness of almost 2 s TWT along the primary F1-fault. This fault defines the SE-border of FNH and has the largest vertical throw (2.5–2.7 s TWT) observed along a single fault plane within the study area. Note that the FFS-1 fault block rotation has previously been interpreted to be of Palaeogene age (Chalmers & Pulvertaft 2001; Sørensen 2006), while this study shows evidence of important fault block rotation already during the early Campanian and deposition of the Kangeq Sequence (see Section 4.5). The FFS-1 faults were reactivated during the mid-late Palaeocene following a significant phase of uplift and erosion in the latest Cretaceous–early Palaeocene (Base Cenozoic Unconformity).

initiated already in the earliest Campanian during deposition of the Kangeq Sequence, that is, contemporaneous with the ongoing post-rift subsidence over the NW/NNW-striking Lower Cretaceous rift basins (*cf.* Section 4.4). This interpretation contradicts with the proposed Palaeogene age of the structures (e.g. Chalmers & Pulvertaft 2001). The figure shows four seismic subunits (KS1–KS4) which have been interpreted within the Kangeq Sequence. The uppermost KS4 only exists in the deeper parts of FFS-1 due to angular truncation over the F1-footwall block, while KS1–KS3 can be traced from the main F1-footwall block and into the hangingwall block. The internal reflections of KS1–KS4 show weak divergence towards the F1-fault and the total thickness of KS1–KS3, which constitutes the entire interval of lower Campanian mudstone in Q-1, increases from 0.5 s TWT in Q-1 to almost 1.5 s TWT in the hangingwall block. This indicates that important fault block rotation in FFS-1 took place already during deposition of KS1–KS3, that is, the lower Campanian Kangeq Sequence represents a fully marine syn-rift sequence with regard to the NNE-striking FFS-1. This interpretation correlates well with interpretations of fault activity in the Nuussuaq Basin onshore West Greenland (see Fig. 1 for location), where important faulting started in early-Campanian time and was resumed in mid-Maastrichtian time (Dam *et al.* 2000).

Like FFS-1, the lower Campanian Kangeq Sequence constitutes the main sedimentary infilling of FFS-2 (Fig. 10d). Thus, the sim-

ilarity in strike and sedimentary infill indicates that FFS-2 and FFS-1 are parts of an integrated rift basin that initiated by lower Campanian rifting. However, contrary to the pronounced normal-slip within FFS-1, the geometry of FFS-2 suggests a significant strike-slip component. A sinistral slip is here favoured considering the regional kinematics along the parallel fault zones (e.g. Ungava Fault Zone) in the Davis Strait and based on the seismic interpretation of a possible restraining bend (push-up-structures and deformed basement) to the northwest of FFS-2 (see Fig. 6 and Section 6.1).

The lower Campanian extension to sinistral transtension in FSC caused renewed deepening in the NW/NNW-striking PB (Figs 10c and 11c) and partly in the NNW-striking FEB (Fig. 10b). Similar reactivated Lower Cretaceous rift basins have been interpreted elsewhere offshore southern West Greenland (Sørensen 2006).

#### 4.6 Latest Cretaceous to mid-late Palaeocene uplift and erosion

The Late Cretaceous marine regime in FSC was terminated by significant uplift during the latest Cretaceous–mid-late Palaeocene. The uplift resulted in deep erosion and widespread angular truncation of the Kangeq Sequence against the Base Cenozoic Unconformity (e.g. Figs 4, 7 and 8) and in complete removal of Upper

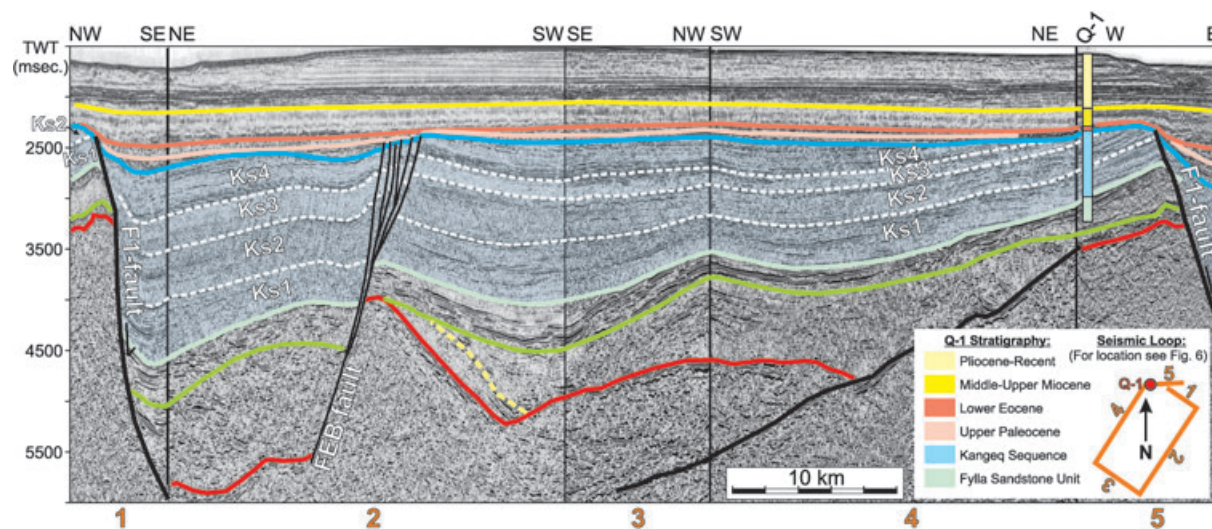


**Figure 9.** Time migrated MCS merged profile of five seismic sections (1–5) that extend from the F1 footwall block of FFS-1 and into its main hangingwall block, circumventing the large vertical throw of the F1-fault. Q-1 was drilled into crest of the F1 footwall block and ties with the loop. See Fig. 6 for location. See Fig. 2 for colour coding of the interpreted seismic horizons. The seismic profile shows evidence for important early Campanian fault block rotation in FFS-1. KS1–KS4 represent interpreted subunits in the Lower Campanian Kangeq Sequence (transparent blue) of which KS1–KS3 represent the entire Lower Campanian interval in Q-1, while KS4 is only present in the F1-hangingwall due to truncation. No evidence is seen of thickening of the Fylla Sandstone Unit across the F1-fault (or the other FFS-1 faults; see Fig. 8). In contrast, pronounced differentiated thickening is observed of KS1–KS3 across the F1-fault indicating early Campanian syn-rift deposition. Note the NE-/E-directed onlap pattern of the Kangeq Sequence over the F1-footwall block indicating syn-rift uplift along F1.

Cretaceous sediments and exposure of pre-Cretaceous basement over the shallowest parts of FWH and FNH (Figs 10a and 11c). The uplift has been mapped in the entire southern and central West Greenland basin (Fig. 2) and linked with an impact of the Icelandic mantle plume around chron 27N (early Palaeocene), eruption of extensive flood basalts in West Greenland (*ca.* 61–59 Ma) and onset of true seafloor spreading in the Labrador Sea (*cf.* Section 2.1).

#### 4.7 Cenozoic drift and post-drift development

The structural configuration of FSC at the end of the Cretaceous was only slightly altered during the Cenozoic drift and post-drift phases and this by a late Palaeocene rift phase, which mainly reactivated and deepened the NNE-striking faults of FFS-1 (Figs 8 and 11d). Hence, no new structural segments were formed during the Cenozoic, which was dominated by deposition of marine mudstones interrupted by periods of uplift and erosion (see Figs 4 and 11d–f).

### 5 CRUSTAL STRUCTURE FROM GRAVITY MODELLING

The study area is characterized by relatively small Free-air gravity anomalies ranging from –20 mGal over the deep rift basins to 25 mGal over the basement highs (Fig. 12). This indicates that the structures are partly compensated at depth (Blakely 1996). In contrast, the pronounced 90 mGal anomaly located along the southern West Greenland Shelf marks the shallow density contrast between a thick ocean layer over Fylla Bank and adjacent young (uncompensated) sediments beneath the shelf. This is a typical feature for Arctic continental margins (Vogt *et al.* 1998). Note that the regional gravity (Fig. 1) shows that FSC is situated in a ‘wedge’ between the NNW-striking positive shelf anomaly to the north/northeast and a NW-striking negative anomaly to the south/southwest; that is, the Lower Cretaceous NNW- and NW-striking structural trends of FSC

(Fig. 6) are also present in the regional gravity anomaly pattern along the margin indicating a close structural–tectonic relationship.

The 630-km-long, WSW–ENE-trending NUGGET Line 1 wide-angle seismic profile in the northernmost Labrador Sea transects FSC and ties with Q-1 at its ENE-end (see Figs 1 and 12 for location). The seismic *P*-wave velocity model (Fig. 13), published in Funck *et al.* (2007), shows that FSC is underlain by a three-layered, laterally homogeneous continental crust consisting of (i) a 1–4-km-thick upper crust with *P*-wave velocities of 5.4–5.6 km s<sup>–1</sup>, the upper crust being thinnest beneath FCB and FFS-1, (ii) a middle crust of 8–10 km thickness with velocities of 6.35–6.55 km s<sup>–1</sup> and (iii) a lower crust of 4–9 km thickness with velocities of 6.6–6.8 km s<sup>–1</sup>; the total crust being thinnest (12 km) beneath FFS-1 and thickest (17 km) beneath FWH. The crust is bounded above by sediments with velocities of 1.6–4.4 km s<sup>–1</sup> and below by an upper mantle with velocities of 7.9 km s<sup>–1</sup>. Note the 5 km Moho uplift beneath FFS-1.

#### 5.1 Pseudo-3-D gravity modelling

The 150-km-long Fylla part of the NUGGET Line 1 seismic velocity profile was adapted for detailed 2.5-D gravity modelling (see Supplementary Information, Part 2) for subsequent use of the modelled best fit sedimentary, crustal and upper-mantle densities in a 3-D crustal structure evaluation of the entire FSC. A pseudo-3-D residual gravity modelling technique (Donato & Tully 1981; Zervos 1987) was applied along eight, 50–135-km-long and intersecting NW–SE- and NE–SW-oriented lines (see Fig. 12 for location). The modelling procedure was as follows: First, the 2.5-D gravity response of the seabed and the sedimentary structures along the profiles was modelled using the best fit densities obtained along NUGGET Line 1 (see Fig. S2). The long-wavelength gravity response of the remote seabed was furthermore constrained several tens of kilometres beyond the seismic reflection study area from bathymetry data (see Fig. 12). To reduce the corresponding, remote

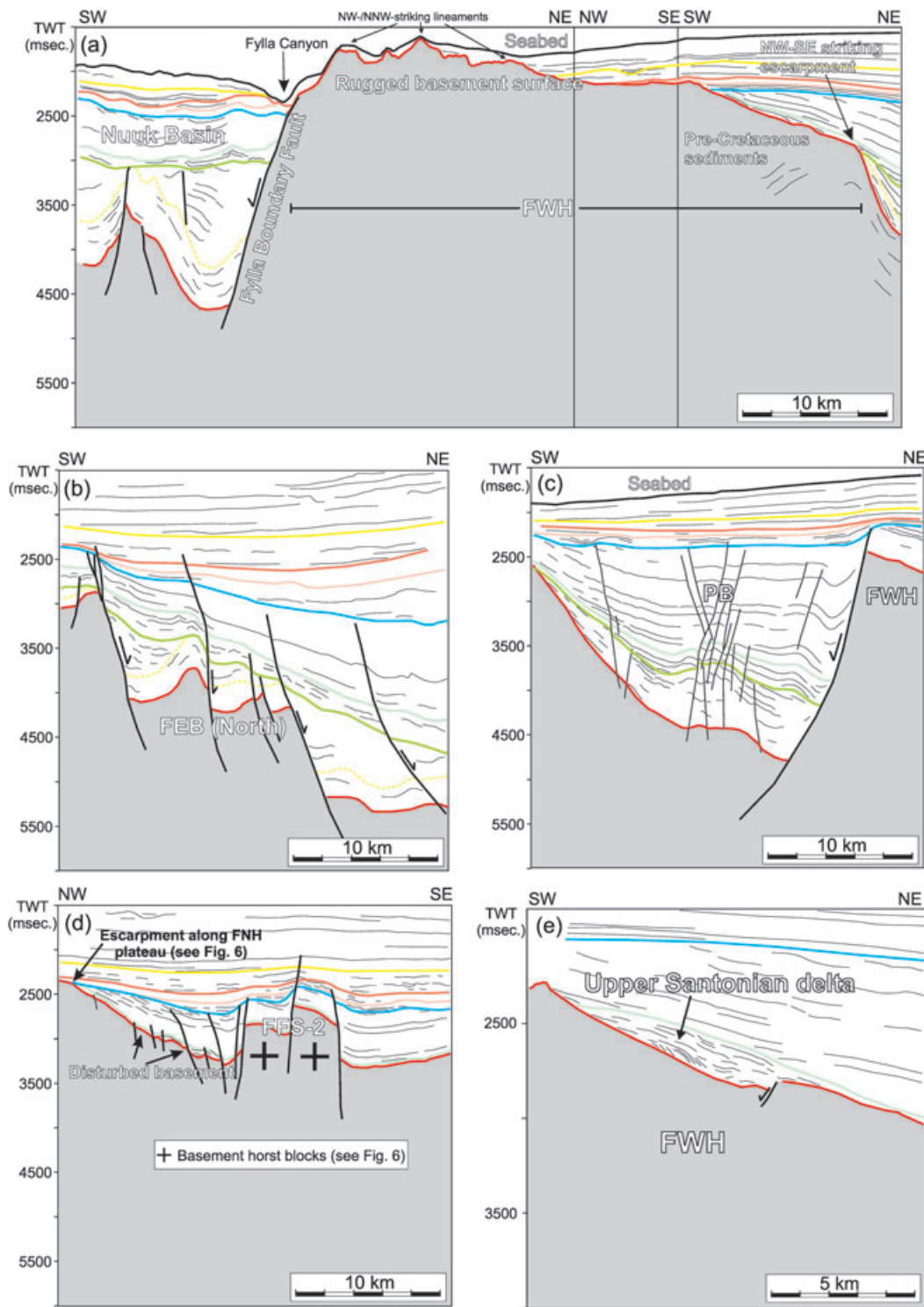
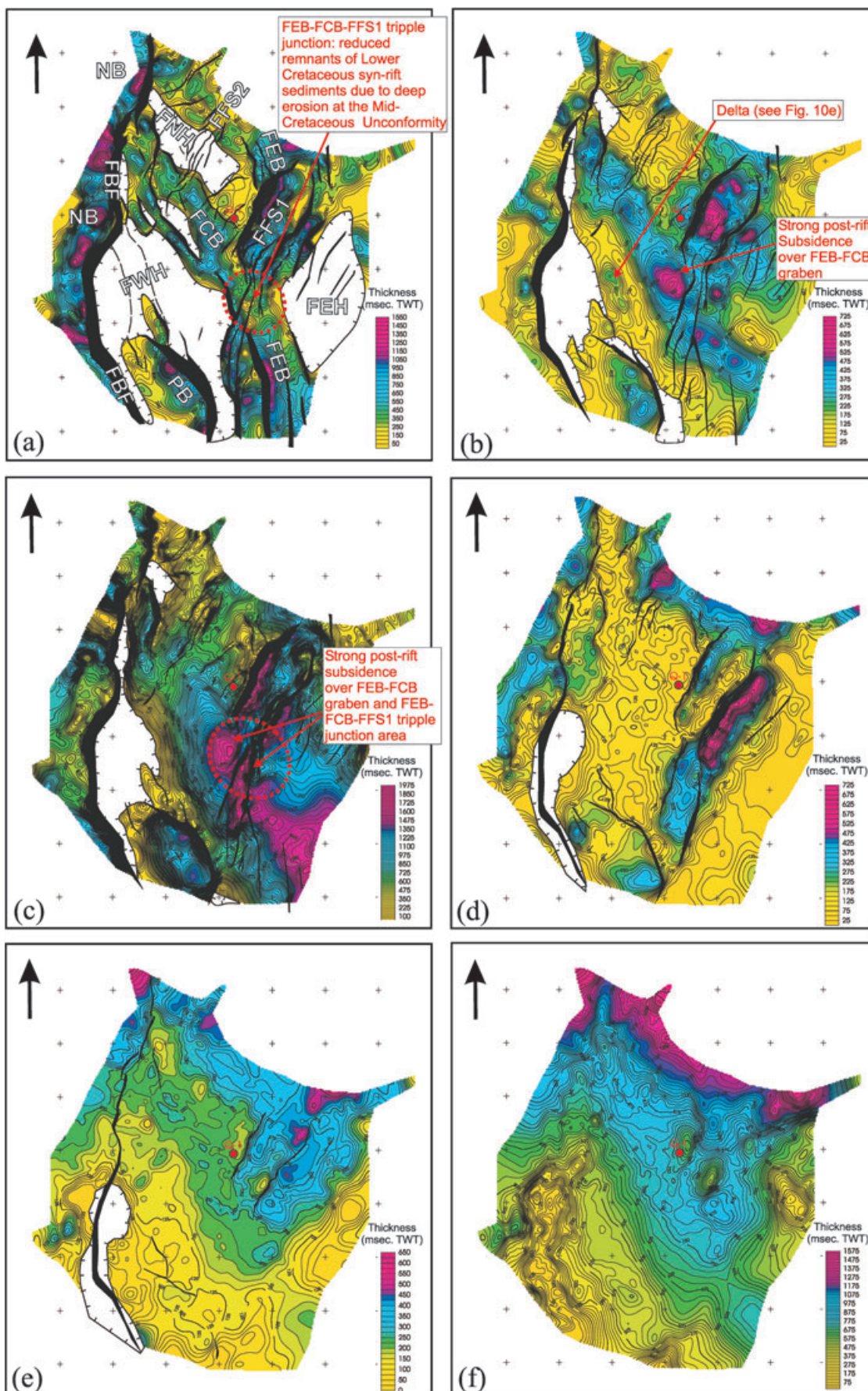


**Figure 10.** Line drawings of MCS profiles showing the variability in mapped structures in FSC. See Fig. 6 for location of profiles. See Fig. 2 for colour coding of the interpreted seismic horizons. Uninterpreted seismic profiles are shown in Supplementary Information, Part 1. (a) Profile across Fylla West High (FWH), Fylla Boundary Fault (FBF) and part of the deep Nuuk Basin to the W/SW of FSC. Note the NW/NNW-striking basement lineaments over FWH. Evidence of pre-Cretaceous sediments are seen beneath FWH on the uninterpreted seismic profile (Fig. S1a). (b) Profile across the northern part of the NNW-striking Fylla East Basin (FEB). (c) Profile across the NW/NNW-striking Paamiut Basin (PB). The oldest sediments infilling PB are interpreted to correlate with the Lower Cretaceous pre- and syn-rift Kitsissut and Appat Sequences in FEB and FCB. This is based on the similar rift-orientations of PB, FEB and FCB and the interpretation that the pre- and syn-rift units in PB are truncated against the Mid-Cretaceous Unconformity. In contrast to FEB and FCB, however, the lower Campanian Kangeq Sequence constitutes the main syn-rift infill in PB indicating significant fault-reactivation and deepening during the early Campanian. (d) Profile across the NNE-striking Fylla Fault System-2 (FFS-2). A strike-slip component is interpreted in FFS-2 based on the overall anastomosing fault pattern, the nearly vertical nature of the faults and the confinement of the faults to a very narrow zone. This is supported by the observation of basement push-up structures to the northwest of FFS-2 (see Fig. 6). (e) Upper Santonian delta over the NE-dipping and deepest part of FWH.



long-wavelength effects of the Moho interface, the seabed outside FSC was used to obtain a first-order fit of this density interface here, assuming a strong correlation (spectral coherence  $>0.5$ ) between variations in seabed and the observed gravity field for wavelengths between 15 and 160 km. For an area in almost isostatic compensation (see Fig. 1), the remainder of the long-wavelength field ( $>160$  km) after subtracting the gravity effect of the seabed is mainly attributed to the Moho density interface (e.g. Smith & Sandwell 1994; Døssing *et al.* 2010b). Secondly, the response of the seabed and sediments as constrained from the seismic reflection interpretations was subtracted along the eight profiles. Subsequently the long-wavelength part of the residual gravity anomaly was fitted by the Moho density interface, following a differentiation of the crust into upper, middle and lower crustal density intervals constrained from NUGGET Line 1. This differentiation was done to get a more realistic vertical density distribution. Finally, a pseudo-3-D gravity modelling procedure was applied by tying the eight 2-D density models to each other and to the NUGGET Line 1 model in a grid until a minimum error was obtained at all intersections. Note that it was not attempted to model short-to-intermediate wavelength misfits along the eight profiles by adding lateral intracrustal density variations since these were unresolved by the NUGGET Line 1 velocity profile (see Fig. 13). Also, the purpose of the applied pseudo-3-D modelling was to obtain a first-order model of the Moho beneath FSC.

The eight 2-D density models (Figs 14a–g) show a reasonable gravity fit to the observed anomalies and in particular when modelling the long profiles (Figs 14a–c and e). A  $-10$  mGal misfit is observed along profiles M–N (Fig. 14f) and O–P (Fig. 14g) in the intervals 50–80 km and 50–65 km, respectively. The cause of these misfits is likely related to out-of-plane effects, since corresponding misfits are not observed at the crossing profiles A–B (Fig. 14a) and C–D (Fig. 14b). Note that the short-wavelength anomalies of the calculated gravity response generally do not correlate very well with the observed and relatively smooth anomalies (e.g. Fig. 14a: 60–70 km and Fig. 14d: 30 km). This discrepancy is related to the fact that the observed gravity anomalies were extracted from a gridded satellite data set. Note also that the modelling is associated with some uncertainty resulting from the assumption of laterally homogeneous intracrustal layers. This uncertainty may be estimated assuming that the maximum applied intracrustal layer density shifts from NUGGET Line 1 ( $\pm 50$  kg m $^{-3}$ ) (see Supplementary Information, Part 2) also represents the expected lateral intracrustal layer density variation along the remaining eight profiles. This assumption is valid considering that the NUGGET Line 1 profile transects most of the structures in FSC (see Fig. 6). Thus, if the  $\pm 50$  kg m $^{-3}$  density

**Table 1.** Abbreviations used for mapped structures in the Fylla area.

Fylla Boundary Fault	FBF
Fylla Central Basin	FCB
Fylla East Basin	FEB
Fylla East High	FEH
Fylla Fault System	FFS
Fylla North High	FNH
Fylla Structural Complex	FSC
Fylla West High	FWH
Nuuk Basin	NB
Paamiut Basin	PB
Qulleq-1	Q-1

variations are assumed to be located within the total 4–12-km-thick upper and middle crustal layers (i.e. similar to NUGGET Line 1), the assumption of laterally homogeneous intracrustal layers along the eight profiles corresponds to an error in the modelled Moho depth of maximum 0.6–1.6 km using a density contrast of 320 kg m $^{-3}$  at the Moho interface.

## 6 DISCUSSION

### 6.1 Crustal and upper-mantle syn- and post-rift dynamics

The Cretaceous syn- and post-rift crustal and upper-mantle dynamics in FSC are here discussed based on compiled maps of the (i) top pre-Cretaceous basement depth (Fig. 15a), (ii) total Upper Cretaceous sedimentary thickness (Fig. 15b), (iii) Moho depth (Fig. 15c) and (iv) crustal thickness (Fig. 15d). The total Upper Cretaceous thickness is shown because it reflects the early (late Santonian) to late (early Campanian) post-rift stages with regard to the Lower Cretaceous rift basins (*cf.* Section 4.4), that is, this thickness provides direct insight into the post-rift-related crustal-mantle dynamics during Late Cretaceous time.

In general, the maps reveal a strong correlation between basement and Moho depths and the thickness of Upper Cretaceous sediments and the crust. Thus, the three basement highs (FWH, FNH and FEH) are characterized by shallow basement (Fig. 15a), a deep Moho (Fig. 15c) and a thick crust (Fig. 15d); the basement being shallowest (1.5 km), the Moho deepest (24 km) and the crust thickest (22 km) beneath FWH. These observations correlate well with the absence or only thin layer of Upper Cretaceous post-rift sediments here (Fig. 15b). Note that the FWH basement progressively shallows

**Figure 11.** Isochore maps of interpreted seismic units. See Table 1 for abbreviations used. (a) Undifferentiated pre- and syn-rift Lower Cretaceous (Kitsissut and Appat Sequences). Note that Lower Cretaceous sediments are missing over FWH, FNH and FEH due to erosion at the Mid-Cretaceous Unconformity. (b) Upper Santonian Fylla Sandstone Unit. The early post-rift depocentre was mainly confined over the axes of the Lower Cretaceous rift basins with prograding deltas developing over the adjacent basement highs (see Fig. 10e). (c) Lower Campanian Kangeq Sequence. The lower Campanian marine mudstones represent a phase of broad tectonic subsidence but with deposition being concentrated over the Lower Cretaceous rift basins and within the hangingwall blocks of FFS-1 and PB. Note the marked thickening of the Kangeq Sequence (Fig. 11c) in the triple junction area, reflecting strong Late Cretaceous post-rift subsidence in this area. Lower Campanian sediments are missing over large parts of FWH and FNH due to erosion at the Base Cenozoic Unconformity. (d) Total Palaeogene (upper Palaeocene and lower Eocene). The Palaeogene represents two phases of tectonic subsidence separated by a relative sea level fall and widespread erosion of upper Palaeocene sediments during the earliest Eocene (Palaeocene–Eocene Unconformity). Note the Palaeogene thickening in FFS-1 which reflects reactivation of the NNE-striking faults, mainly in the late Palaeocene. The thickening in the northernmost part of the area reflects a Cenozoic depocentre that was established in the Palaeocene. (e) Middle–Upper Miocene. From Middle Miocene time the northern depocentre deepened with deposition of thick marine mudstones. At the end of Miocene a minor relative sea level fall resulted in reexposure of pre-Cretaceous basement over parts of FWH (see Figs 2 and 10a). (f) Pliocene–Recent. During the Pliocene–Quaternary, FSC was permanently flooded and thick sediments were deposited in SW-prograding clinoforms to the north.

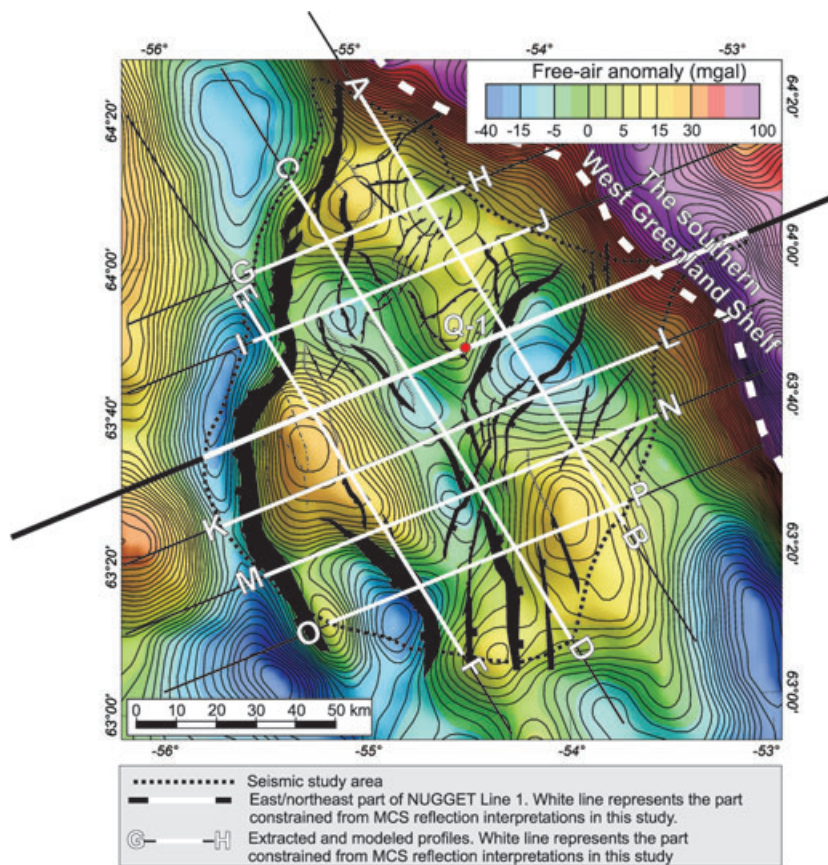


**Figure 12.** Map of  $5 \times 5$  km gridded free-air gravity anomalies (Andersen & Knudsen 1998). The mapped structures from seismic (Fig. 6) are superposed on the map. Also shown are lines used in pseudo-3-D gravity modelling. The bold white part of the lines shows the extent to which sedimentary horizons were constrained from seismic reflection interpretations. The black extreme parts of the lines represent the extent to which a first-order fit was obtained of the Moho from seabed (see text for details). See Fig. 1 for full extent of NUGGET Line 1.

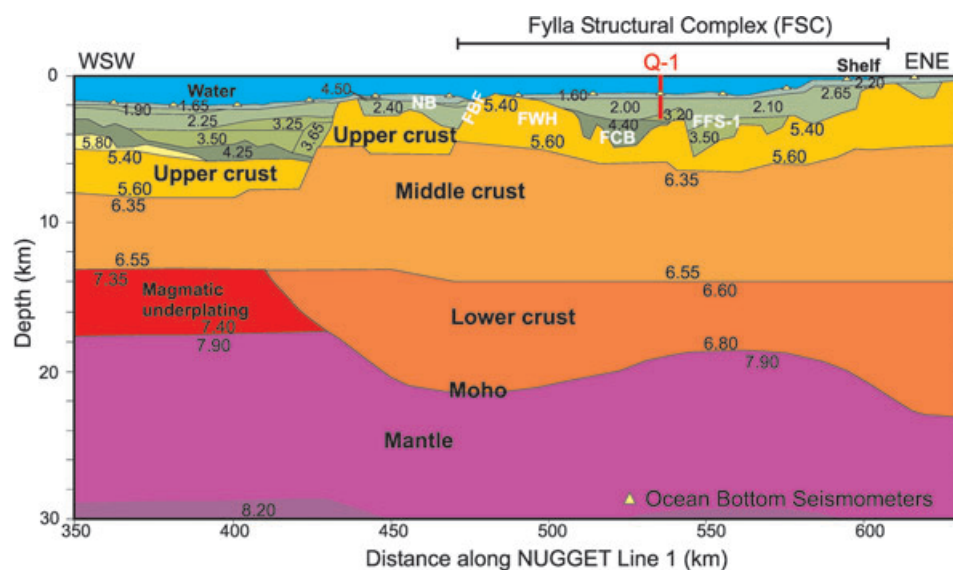


**Figure 13.** NUGGET Line 1 velocity model (Funck *et al.* 2007). Note that only the easternmost  $\sim 300$  km of the total velocity profile is shown. Numbers in the blocks refer to  $P$ -wave velocity in  $\text{km s}^{-1}$ . See Figs 1, 6 and 12 for location of NUGGET Line 1. See Table 1 for abbreviations used. Only significant velocity contrasts were modelled and individual layers were modelled with a constant and smoothed velocity gradient throughout the layer (T. Funck, GEUS, personal communication, 2007). Thus, the interpreted pre-Cretaceous sediments beneath FWH (see Fig. 10a) are not differentiated from the underlying crystalline upper crust. This may be because the pre-Cretaceous sediments are carbonate rocks (*cf.* Section 3.2). Note the 5 km Moho uplift beneath FFS-1 in the central part of FSC.

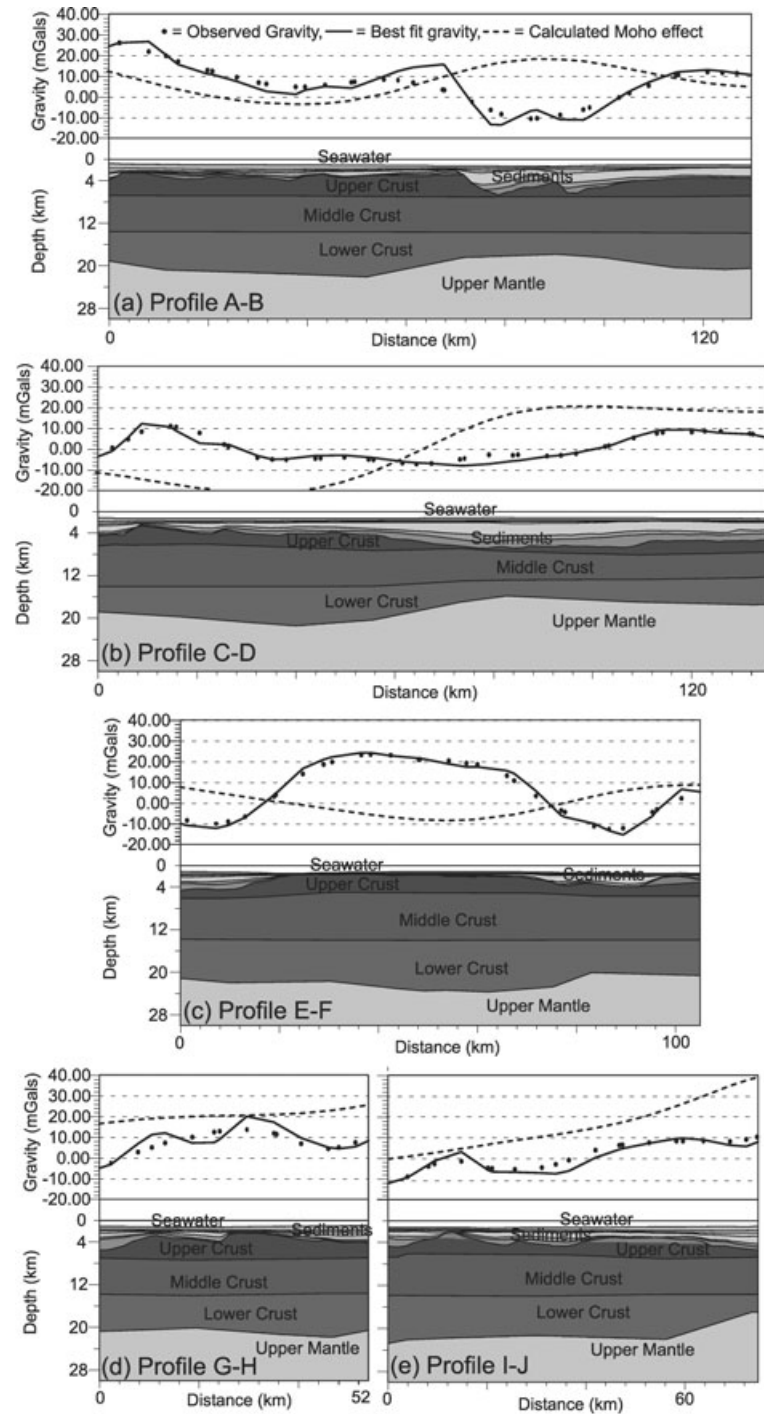


**Figure 14.** Results of pseudo-3-D gravity modelling along eight NW-SE- and NE-SW-oriented lines. The lines constitute together with NUGGET Line 1 a rectangular net with approximately  $20 \times 20$  km grid resolution (see Fig. 12 for location of the lines). Structural models of the sedimentary layers and the Top pre-Cretaceous basement were extracted along the lines from time-to-depth converted and gridded seismic horizons (see Supplementary Information, Part 2). Free-air gravity anomalies were extracted from the gridded satellite gravity data (Fig. 12). Note that a maximum Moho topography of  $\sim 8$  km within FSC is modelled along profile K-L (Fig. 14f). Here, the Moho shallows from 24 km beneath FWH (Fig. 14f: 20 km) to 16 km beneath FFS-1 (Fig. 14f: 70 km).

to the southwest towards FBF (Figs 10a and 15a), suggesting that FWH was isostatically uplifted and tilted by downfaulting in the adjacent NB.

The intervening NNW-, NW- and NNE-striking rift basins (FEB, FCB, PB and FFS-1) are characterized by a deep basement (Fig. 15a), a shallow Moho (Fig. 15c) and a thin crust (Fig. 15d).

The shallowest Moho depth (16 km) and thinnest crust (11 km) are found in the triple junction area between FEB, FCB and FFS-1. This area is also characterized by the maximum thickness of Upper Cretaceous sediments of more than 3.5 km (Fig. 15b). Importantly, only thin remnants of Lower Cretaceous rift sediments are preserved here (see Fig. 11a), which was interpreted as

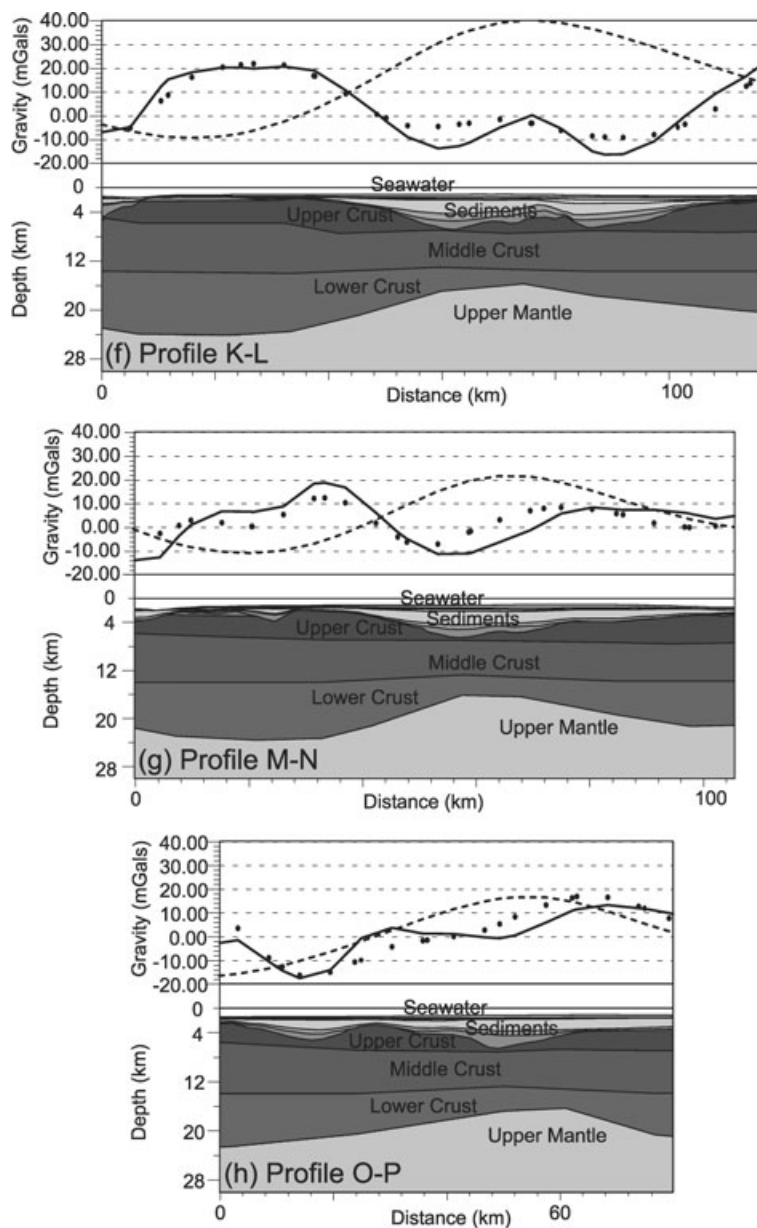


Figure 14. (Continued.)

evidence of strong rift-induced thermal uplift and deep erosion at the Mid-Cretaceous Unconformity (*cf.* Section 4.3). The NNE-striking faults of FFS-1 that transect the triple junction area display only minor fault slip. Hence, the thick Upper Cretaceous sediments in this area are predominantly post-rift sediments related to late-Early Cretaceous crustal attenuation in FEB and FCB. The interpretations indicate that the axis of the Upper Cretaceous post-rift sag basins generally coincides with the zone of maximum lithospheric attenuation. This favours a prevailing pure shear stretching model for FSC in which Cretaceous basin dynamics were largely attributed to the amount of crustal attenuation, the magnitude of the induced thermal anomaly and the subsequent cooling and contraction of this anomaly (*cf.* McKenzie 1978; White & McKenzie 1988; Ziegler & Cloetingh 2004). However, despite that significant extension was interpreted within FCB (*cf.* Section 4.2, Fig. 7), this basin is characterized by only 1.5-km-thick post-rift sediments (Fig. 15b) and

a relatively thick crust of ~18 km (Fig. 15d). This suggests that crustal attenuation in FCB was displaced by the low-angle detachment plane in a prevailing simple-shear type rifting (*cf.* Wernicke 1985).

## 6.2 Crustal attenuation

Results of seismic refraction experiments (Mooney & Braile 1989) and receiver-function analysis (Dahl-Jensen *et al.* 2003) show that the crustal thickness of the unstretched Archean craton in the Labrador region and in southern Greenland is roughly 35 km. This indicates a total (uniform) crustal attenuation ( $\beta$ ) of 1.6–3.2 for the 11–22-km-thick crust in FSC (Fig. 16a). However, indications of a major late Palaeozoic sedimentary basin between Greenland and Canada (Rolle 1985) and a possible Mesozoic seaway

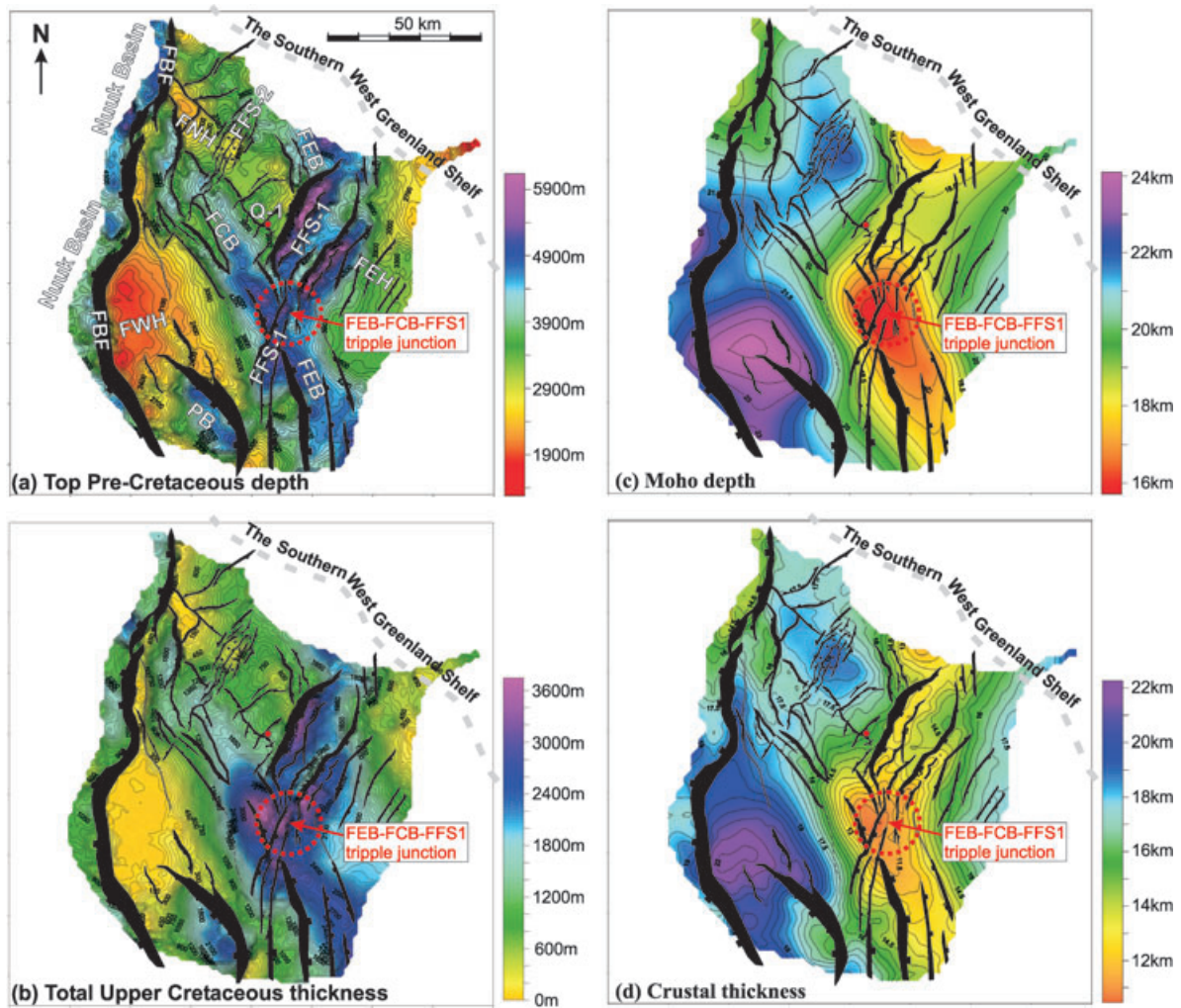


**Figure 15.** Maps reflecting the Cretaceous syn- and post-rift basin dynamics in FSC. The mapped basement structures (see Fig. 6) are superposed on the maps. See Table 1 for abbreviations used. (a) Top pre-Cretaceous basement depth. (b) Total Upper Cretaceous sedimentary thickness (Fylla Sandstone Unit and Kangeq Sequence). (c) Moho depth. (d) Crustal thickness. The Moho map was compiled using the results of the pseudo-3-D gravity modelling (Fig. 14), while the crustal thickness was obtained by subtracting the Top pre-Cretaceous basement depth from the Moho depth, that is, the crustal thickness includes possible remnants of pre-Cretaceous sediments (Lower Palaeozoic carbonates?) overlying the true crystalline basement. These pre-Cretaceous sediments may have deformed differently than the underlying crystalline crust and thus have had a potential tectonic influence during the Cretaceous rifting. Note the right-stepping *en echelon* pattern of deep basement, thick Upper Cretaceous sediments, shallow Moho and thin crust along the southern part of FEB, FFS-1 and the northern part of FEB. Note also the very thin crust and thick Upper Cretaceous sediments in the triple junction area of FEB, FCB and FFS-1.

(Bojesen-Kofoed *et al.* 2004) suggest that the pre-Cretaceous crustal thickness in FSC was less than 35 km. Assuming that the 22-km-thick crust beneath FWH remained almost unaffected by Cretaceous rifting, and thereby represents a more realistic pre-rift crustal thickness of FSC, the maximum values of  $\beta$  for the late-Early Cretaceous rift phase (i.e. in the triple junction area) are therefore likely to be closer to 2.0 (Fig. 16b). However, despite the significant rifting in FSC, the seismic reflection data show only few indications of intrasedimentary sills. Bown & White (1995) show that no melt is produced above a normal temperature asthenosphere (1300°C) for  $2.0 \leq \beta \leq 3.2$  if extension took 5 Myr or more due to conductive loss of heat. This condition appears to have been complied for the late-Early Cretaceous rifting in FSC; an interpretation which correlates well with the sparse evidence of Early Cretaceous syn-extensional volcanism elsewhere on the southern West Greenland Shelf (e.g. Chian & Loudon 1992; Chalmers 1997; Chalmers & Pulvertaft 2001).

### 6.3 Structural-kinematic rift model (poly-phase rifting in FSC)

The seismic mapping (Fig. 6; Section 4) indicates that FSC formed under strong influence of the lithospheric stresses that acted in both the overall NW-striking Labrador Sea and in the N-/NNE-striking, Ungava Fault Zone (sub)parallel rift basins in the Davis Strait (see Fig. 1). Thus, the dominance of NW-/NNW-striking faults in the southern part of FSC can be linked with break-up stresses in the Labrador Sea, while the dominance of NNE-striking faults mainly to the north can be linked with stresses in the Davis Strait. However, the structural configuration of FSC (Fig. 6) and the variety of structural styles (Figs 5 and 7–10) suggest some kind of additional pre-rift basement control, and that the structural outcome was not just the result of poly-phase rifting and changes in orientation of the stresses. Thus, the geometry of rifts is often strongly influenced by pre-existing basement fabric acting as crustal weakness zones that

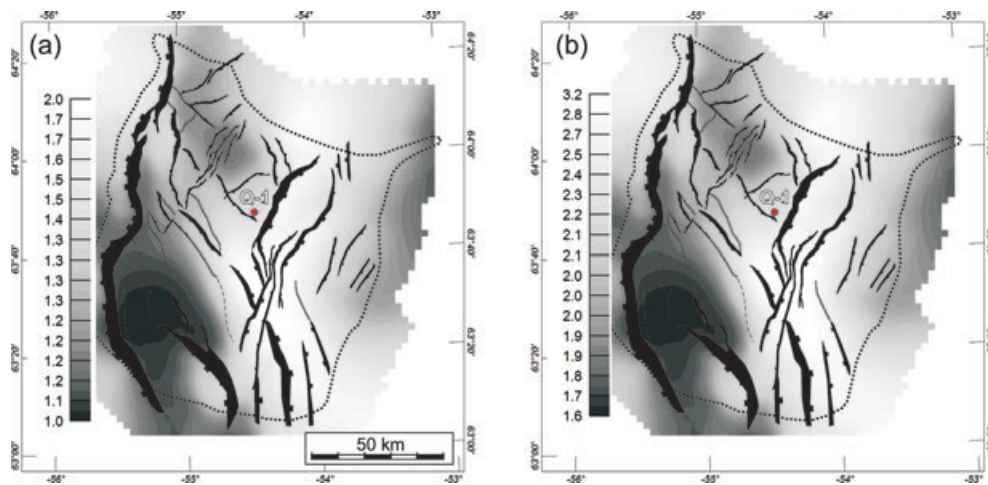


**Figure 16.** Maps of crustal attenuation. The mapped basement structures (see Fig. 6) are shown on the maps. See Table 1 for abbreviations used. (a) Total crustal attenuation assuming a pre-rift crustal thickness of 35 km similar to unstretched crust in southern Greenland. (b) Crustal attenuation for the Cretaceous rift assuming a pre-rift crustal thickness of 22 km. Maximum attenuation of 2.0 is found in the triple junction area which primarily was affected by late-Early Cretaceous rifting. High attenuation values ( $>1.5$ ) are also found in the FFS-1 area, where NNE-striking structures initiated transensional transfer faults during the late-Early Cretaceous rifting and later developed major fault blocks (FFS-1) during the early Campanian and late Palaeocene E–W/ENE–WSW extension.

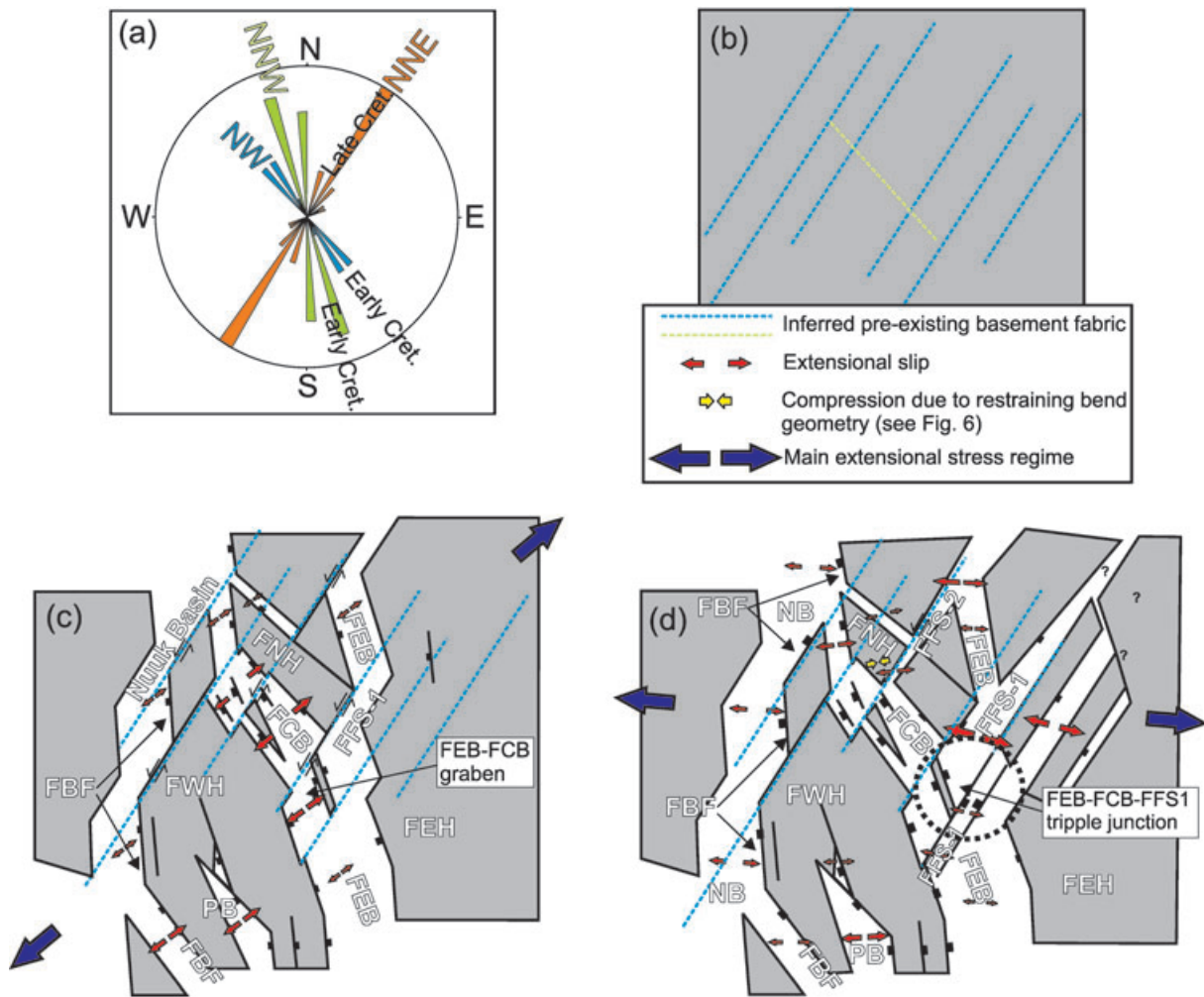
can be reactivated at stress levels considerable below the bulk yield strength of homogeneous crust (e.g. Pinet & Colletta 1990; Ziegler & Cloetingh 2004). In particular, it can be speculated whether rifting in FCB nucleated along a pre-existing low-angle weakness zone as expressed by the SW-dipping detachment plane beneath the basin (Figs 6 and 7). Also, the right-stepping *en echelon* offset of the NNW-striking FEB along the NNE-striking FFS-1 (Fig. 6) may indicate a pre-rift NNE-striking basement fabric, which initiated transensional transfer faults during the Early Cretaceous rifting. This may also explain the pattern of alternating NNW- and NNE-striking fault segments along FBF (Fig. 6; Section 4.1). Moreover, the western bathymetric border of Fylla Bank, as outlined by the deep NNE–N-striking Fylla Canyon, correlates with the structural trend of the underlying NB (see Figs 3 and 6) and with along-strike discontinuities (N–/NNE-striking transfer faults) observed in oceanic crust in the Labrador Sea (see Fig. 1). Similar interpretation may be valid for the deep canyon that borders Fylla Bank to the east outside the seismic study area. Hence, the NNE-striking fabric possibly defines a segmentation of the margin. Correlations between the pattern of margin segmentation and that associated with along-strike discontinuities (e.g. Macdonald 1982) observed at mid-ocean ridges have also been made by Behn & Lin (2000). Whether the NNE-striking fabric in the Fylla area is inherited from older rifting/basement structures is difficult to say.

Fig. 17 shows a structural-kinematic rift model for FSC based on the discussion, the seismic and gravity interpretations, and a simple palaeostress analysis of 72 primary fault segments within FSC (Fig. 17a). The latter assumes a correlation between palaeostress direction and fault characteristics such as strike, slip-type and cross-sectional seismic expression. Following the initial pre-rift setting (Fig. 17b), an overall WSW–ENE to SW–NE directed extensional stress regime in the late-Early Cretaceous induced rifting and half-graben formation along the NNW–/NW-striking FEB, FCB, PB and FBF, while rifting was accommodated by oblique-shearing along the NNE-structures of FFS-1 (and the NNW-striking segments of FBF) (Fig. 17c). After a period of uplift and erosion in the Mid-Cretaceous, the extensional stress rotated clockwise to an overall

E–W/ENE–WSW direction in the beginning of early Campanian (Fig. 17d). This caused various degrees of sinistral transension along the NNE-striking faults of FFS-1 and FFS-2; the FFS-1 being dominated by pronounced fault-block rotation while strike-slip dominated in FFS-2. The new stress regime also caused significant reactivation in the Lower Cretaceous PB and minor reactivation of the faults in FEB. Similar poly-phase rifting and reactivation of older structures has been interpreted at the west Galicia rifted margin (Reston 2005) and in the Northern North Sea (Tomasso *et al.* 2008). However, the structures in FSC formed as the results of significantly different stress orientations. Thus, the interpreted Cretaceous, clockwise rotation of the stress field from an initial WSW–ENE/SW–NE direction to an E–W/WNW–ESE direction correlates well with regional stress directions interpreted by, for example, Chalmers *et al.* (1993), Balkwill *et al.* (1990) and Faure *et al.* (1996). The rotation relates to the transition from Early Cretaceous continental break-up in the Labrador Sea to increased extensional rifting in the Baffin Bay region (Fig. 1) during the Late Cretaceous and the beginning of the east-directed movement of Greenland away from North America (Whittaker *et al.* 1997; Harrison *et al.* 1999).

#### 6.4 Comparison with other normal-to-shear rifted margins

The seismic and gravity evidence presented in this and other studies (e.g. Funck *et al.* 2007) shows that FSC represents a 120–150-km-wide OCT zone off the southern West Greenland Shelf. The interpreted margin segmentation into series of rift and transform-type structures by NNE-oriented lineaments (Fig. 17) is suggested to be related kinematically to NNE-oriented transfer faults in the Labrador Sea oceanic crust and to the NNE-oriented Ungava Fault Zone in the Davis Strait (Section 6.3). Similar margin complexity and segmentation has been interpreted, for example, along the Senja Shear margin in the SW Barents Sea (Faleide *et al.* 1993), the West African margin off Guinea (Wilson *et al.* 2003), the eastern North



**Figure 17.** Structural-kinematic rift model of FSC. See Table 1 for abbreviations used. The model focuses on the Early to Late Cretaceous evolution since the end-of-Cretaceous structural configuration of FSC was only slightly altered during the Cenozoic drift and post-drift phases and this only by late Palaeocene extension, which mainly reactivated and deepened the NNE-striking faults of FFS-1 (see Fig. 11d). Hence, no new structural segments were formed during the Cenozoic. (a) Rose diagram of 72 mapped fault segments, escarpments and basement lineaments that were analysed in terms of orientation and seismic cross-section geometry. The diagram shows a consistent classification into NNW-, NW- and NNE-striking structures. (b) Pre-rift setting with inferred basement fabric. (c) Late-Early Cretaceous rifting: a WSW-ENE-/SW-NE-directed extensional stress regime caused significant rifting in the NW-/NNW-striking FEB, FCB, PB and FBF. Note the right-lateral offset along NNE-oriented basement structures initiating sinistral transtensional transfer faults. (d) Early Campanian rifting: an E-W/ENE-WSW extensional stress regime resulted in pronounced fault block rotation in FFS-1 (and possibly FBF) and sinistral oblique-slip along FFS-2. The extension also caused reactivation of Lower Cretaceous faults in PB. Note that the interpreted Cretaceous rifting patterns correlate well with the calculated crustal attenuation for FSC (see Fig. 16).

Greenland oblique-shear margin (Døssing *et al.* 2010a) and beneath the Demerara Plateau, part of the French Guinea-Northeast Brazil continental margin (Greenroyd *et al.* 2008; Maillard *et al.* 2010). These margins are also located at the transition between normal and shear rifting regimes and their structural evolution controlled by transform fault zones. Similar to Fylla Bank, which outlines the extent of the underlying FSC and possibly formed as a result of the margin segmentation, the Demerara Plateau also constitutes an individual bathymetric feature and a relative wide OCT, which is situated between transform fault zones (Greenroyd *et al.* 2008).

## 7 CONCLUSIONS

(1) Fylla Bank in the northernmost Labrador Sea is situated above the major FSC which formed at the transition between normal

rifting in the Labrador Sea and oblique-shear rifting in the Davis Strait (mainly expressed by the major Ungava Fault Zone).

(2) Seismic reflection interpretations in this study show that FSC is characterized by an up to 5-km-thick Cretaceous–Cenozoic (incomplete) succession above the inferred pre-Cretaceous basement.

(3) Two rift domains have been mapped: NW-/NNW-striking (Labrador Sea parallel) rift basins, which dominate in the southern part of FSC, and NNE-striking (Ungava Fault Zone parallel) rift basins, which dominate in the northern part.

(4) The NW-/NNW-striking rift basins formed as the result of overall SW-NE extension during the late-Early Cretaceous. Following a period of thermally induced uplift and erosion in the mid-Cretaceous, major fault block rotation initiated along NNE-striking structures during E-W/ENE-WSW extension in the early Campanian. This took place contemporaneously with post-rift

subsidence over the NNW/NW-oriented Lower Cretaceous rift basins. The lower Campanian rift basins were reactivated in the late Palaeocene after a period of significant uplift and erosion during the latest Cretaceous to early Palaeocene.

(5) It is suggested here that NNE-striking basement fabric initiated transtensional transfer faults during the late-Early Cretaceous rift phase, since the spatial configuration of the Lower Cretaceous rift basins appear to be controlled by NNE-striking structures. Considering that the NNE-fabric is subparallel to the deep submarine canyons that border Fylla Bank to the west and east, it is suggested that this fabric defines margin segmentation and link with transfer faults observed in oceanic crust in the Labrador Sea.

(6) Compiled maps of depth to basement, thickness of Upper Cretaceous post-rift sediments, Moho depth and crustal thickness (the latter two compiled from results of 2-D and pseudo-3-D gravity modelling) show a significant correlation between the amount of late-Early Cretaceous crustal attenuation and Late Cretaceous post-rift subsidence in the area. This is interpreted to be a result of thermally controlled basin dynamics. Thus, a minimum crustal thickness of only 11 km (crustal attenuation between 2 and 3.2) is found in an area of thick post-rift sediments.

(7) Finally, a presented structural-kinematic model shows the Early to Late Cretaceous evolution of FSC under the influence of interpreted poly-phase rifting and significantly different stress orientations. The model suggests that the evolution of FSC was controlled by pre-existing crustal fabric combined with influences of lithospheric stresses in both the Labrador Sea and in Davis Strait. This resulted in a very complex tectonic setting and the formation of several distinct structural styles.

## ACKNOWLEDGMENTS

The author would like to express his gratitude to N. E. Hamann (DONG Energy, Denmark), K. Andersen (GEUS), T. Dahl-Jensen (GEUS) and L. Stemmerik (Univ. Of Copenhagen), whose comments greatly improved the final manuscript. Thanks also to J. Gerlings and one anonymous reviewer for very constructive reviews. Finally, thanks to TGS-NOPEC, BGR and GEUS for providing the seismic reflection data and to T. Funck (GEUS) for permission to use the NUGGET Line 1 profile. The paper is published with permission from the Geological Survey of Denmark and Greenland (GEUS).

## REFERENCES

- Andersen, O.B. & Knudsen, P., 1998. Global marine gravity field from the ERS-1 and Geosat geodetic mission altimetry, *J. geophys. Res.*, **103**(C4), 8129–8137.
- Balkwill, H.R., McMillan, N.J., MacLean, B., Williams, G.L. & Srivastava, S.P., 1990. Geology of the Labrador shelf, Baffin Bay, and Davis Strait, in *Geology of the Continental Margin of Eastern Canada*, Vol. 2, chapter 2, pp. 293–348, eds Keen, M.J. & Williams, G.L., Geological Survey of Canada, Ottawa.
- Basile, C., Mascle, J., Benkhelil, J. & Bouillin, J.P., 1998. Geodynamic evolution of the Côte d'Ivoire–Ghana transform margin: an overview of Leg 159 results, *Proc. Ocean Drill. Program, Sci. Results*, **159**, 101–110, doi:10.2973/odp.proc.sr.159.048.1998.
- Bate, K.J., Whittaker, R.C., Chalmers, J.A. & Dahl-Jensen, T., 1994. Fylla Complex: possible very large gas reserves off S.W. Greenland, *Oil Gas J.*, **92**, 79–82.
- Behn, M.D. & Lin, J., 2000. Segmentation in gravity and magnetic anomalies along the U.S. East Coast passive margin: implications for incipient structure of the oceanic lithosphere, *J. geophys. Res.*, **105**, 25 769–25 790.
- Bell, J.S. & Howie, R.D., 1990. Paleozoic Geology, in *Geology of the Continental Margin of Eastern Canada*, Vol. 2, pp. 141–165, eds Keen, M.J. & Williams, G.L., Geological Survey of Canada, Geological Survey of Canada.
- Blakely, R.J. 1996. *Potential Theory in Gravity and Magnetic Applications*. Cambridge University Press, Cambridge, 464pp.
- Bojesen-Kofoed, J.A., Nytoft, H.P. & Christiansen, F.G., 2004. Age of oils in West Greenland: was there a Mesozoic seaway between Greenland and Canada? *Geol. Surv. Denmark Greenland Bull.*, **4**, 49–52.
- Bown, J.W. & White, R.S., 1995. Effect of finite extension rate on melt generation at rifted continental margins, *J. geophys. Res.*, **100**, 18 011–18 029.
- Chalmers, J.A. 1991. New evidence on the structure of the Labrador Sea/Greenland continental margin, *J. Geol. Soc., Lond.*, **148**, 899–908.
- Chalmers, J.A. 1997. The continental margin off southern Greenland: along-strike transition from an amagmatic to a volcanic margin, *J. Geol. Soc., Lond.*, **154**, 571–576.
- Chalmers, J.A. 2000. Offshore evidence for Neogene uplift in central West Greenland, *Glob. Planet. Change*, **24**, 311–318.
- Chalmers, J.A. & Laursen, K.H., 1995. Labrador Sea: the extent of continental and oceanic crust and the timing of the onset of seafloor spreading, *Mar. Pet. Geol.*, **12**(2), 205–217.
- Chalmers, J.A. & Pulvertaft, T.C.R., 2001. Development of the continental margins of the Labrador Sea: a review, *Geol. Soc. Land. Spec. Publ.*, **187**, 77–105. doi:10.1144/GSL.sp.2001.187.01.05.
- Chalmers, J.A., Pulvertaft, T.C.R., Christiansen, F.G., Larsen, H.C., Laursen, K.H. & Ottesen, T.G., 1993. The southern West Greenland continental margin: rifting history, basin development, and petroleum potential, in *Petroleum Geology of Northwest Europe: Proceedings of the 4th Conference*, pp. 915–931 ed Parker, J.R., Geological Society, London.
- Chian, D. & Loudon, K.E., 1992. The structure of the Archaean-Ketilidian Crust along the continental shelf of Southwestern Greenland from a seismic refraction profile, *Can J. Earth Sci.*, **29**, 301–313.
- Chian, D. & Loudon, K.E., 1994. The continent–ocean crustal transition across the southwest Greenland margin, *J. geophys. Res.*, **99**, 9117–9135.
- Chian, D., Keen, C., Reid, I. & Loudon, K.E., 1995a. Evolution of nonvolcanic margins: new results from the conjugate margins of the Labrador Sea, *Geology*, **23**(7), 589–592.
- Chian, D., Loudon, K.E. & Reid, I. 1995b. Crustal structure of the Labrador Sea conjugate margin and implications for the formation of nonvolcanic continental margins, *J. geophys. Res.*, **100**(B12), 24 239–24 253.
- Christiansen, F.G., *et al.* 2001. Petroleum geological activities in West Greenland in 2000, *Geol. Greenland Surv. Bull.*, **189**, 24–33.
- Dahl-Jensen, T., *et al.* 2003. Depth to Moho in Greenland: receiver-function analysis suggests two Proterozoic blocks in Greenland, *Earth planet. Sci. Lett.*, **205**, 379–393.
- Dalhoff, F., Chalmers, J.A., Nøhr-Hansen, H., Rasmussen, J.A., Sheldon, E. & Gregersen, U., 2002. A multidisciplinary study of the Palaeogene succession offshore southern West Greenland, *Geol. Greenland Surv. Bull.*, **191**, 90–96.
- Dalhoff, F., Chalmers, J.A., Gregersen, U., Nøhr-Hansen, H., Rasmussen, J. & Sheldon, E., 2003a. Mapping and facies analysis of Paleocene–Mid-Eocene seismic sequences, offshore southern West Greenland, *Mar. Pet. Geol.*, **20**, 935–986.
- Dalhoff, F., Kuijpers, A., Nielsen, T., Poulsen, N.E. & Shipboard Scientific Party, 2003b. Southern West Greenland– Seabed Sampling Project 2003. TTR-13 Cruise Leg 4 and part of Leg 3, *IOC Workshop Report*, **191**, 16–18.
- Dam, G., Nøhr-Hansen, H., Pedersen, G.K. & Sønderholm, M., 2000. Sedimentary and structural evidence of a new early Campanian rift phase in the Nuussuaq Basin, West Greenland, *Cret. Res.*, **21**, 127–154.
- Donato, J.A. & Tully, M.C., 1981. A regional interpretation of north sea gravity data, in *Petroleum Geology of the Continental Shelf of North-West Europe*, pp. 65–75, eds Illing, L.V. & Hobson, G.D., Institute of Petroleum, London.
- Døssing, A., Dahl-Jensen, T., Thybo, H., Mjelde, R. & Nishimura, Y., 2008. East Greenland Ridge in the North Atlantic Ocean: an integrated

- geophysical study of a continental sliver in a boundary transform fault setting, *J. geophys. Res.*, **113**(B10107), doi:10.1029/2007JB005536.
- Døssing, A., Stemmerik, L., Dahl-Jensen, T. & Schlindwein, V., 2010a. Segmentation of the eastern North Greenland oblique-shear margin, *Earth planet. Sci. Lett.*, **292**, 239–253.
- Døssing, A., Olesen, A.V. & Forsberg, R., 2010b. New aerogravity and aeromagnetic anomaly data over Lomonosov Ridge and adjacent areas for bathymetric and tectonic mapping, *AGU Fall Meeting*, San Francisco, CA, 2010 December 13–17, Abstract T31A-2125.
- Faleide, J.I., Vaagnes, E., Gudlaugsson, S.T., 1993. Late Mesozoic–Cenozoic evolution of the south-western Barents Sea in a regional rift-shear setting, *Mar. Pet. Geol.*, **10**, 186–214.
- Faure, S., Temblay, A. & Angelier, J., 1996. State of intraplate stress and tectonism of northeastern North America since Cretaceous times, with particular emphasis on the New England–Quebec igneous province, *Tectonophysics*, **255**, 11–134.
- Funck, T., Jackson, H.R., Loudon, K.E. & Klingelhöfer, F., 2007. Seismic study of the transform-rifted margin in Davis Strait between Baffin Island (Canada) and Greenland: what happens when a plume meets a transform, *J. geophys. Res.*, **112**, B04402, doi:10.1029/2006JB004308, 2007.
- Greenroyd, C.J., Peirce, C., Rodger, M., Watts, A.B. & Hobbs, R.W., 2008. Demerara Plateau: the structure and evolution of a transform passive margin, *Geophys. J. Int.*, **172**, 549–564.
- Harrison, J.C., et al., 1999. Correlation of Cenozoic sequences of the Canadian Arctic region and Greenland: implications for the tectonic history of northern North America, *Bull. Can. Pet. Geol.*, **47**(3), 223–254.
- Isaacson, E.S. & Neff, D.B., 1999. A, B AVO cross plotting and its application to Greenland and the Barent Sea, in *Petroleum Geology of Northwest Europe: Proceedings of the 5th Conference*, pp. 1289–1298, eds Fleet, A.J. & Boldy, S.A.R., *AGU Fall Meeting*, San Francisco, CA, 2010 December 13–17, Abstract T31A-2125.
- Japsen, P., Bonow, J.M., Green, P.F., Chalmers, J.A. & Lidmar-Bergström, K., 2006. Elevated, passive continental margins: long-term highs or Neogene uplifts? New evidence from West Greenland, *Earth planet. Sci. Lett.*, **248**, 315–324, doi:10.1016/j.epsl.2006.05.036.
- Keen, C.E. & Barrett, D.L., 1972. Seismic refraction studies in Baffin Bay: an example of a developing ocean basin, *Geophys. J. R. astr. Soc.*, **30**, 253–271.
- Keen, C.E., Kay, W.A. & Roest, W.R., 1990a. Crustal anatomy of a transform continental margin, *Tectonophysics*, **173**, 527–544.
- Keen, C.E., Loncarevic, B.D., Reid, I., Woodside, J., Haworth, R.T. & Williams, H., 1990b. Tectonic and geophysical overview, in *Geology of the Continental Margin of Eastern Canada*, Vol. 2, pp. 31–85, eds Keen, M.J. & Williams, G.L., Geological Survey of Canada, Ottawa.
- Larsen, L.N., Rex, D.C., Watt, S. & Guise, P.G., 1999. 40Ar/39Ar dating of alkali basaltic dykes along the south-west coast of Greenland: Cretaceous and Tertiary igneous activity along the eastern margin of the Labrador Sea, *Geol. Greenland Surv. Bull.*, **184**, 19–29.
- Loudon, K.E. & Chian, D., 1999. The deep structure of non-volcanic rifted continental margins, *Phil. Trans. R. Soc. Lond., Ser. A*, **357**, 767–800.
- Macdonald, K.C., 1982. Mid-Ocean ridges: fine-scale tectonic, volcanic, and hydrothermal processes with the plate boundary zone, *Ann. Rev. Earth planet. Sci.*, **10**, 155–190.
- Maillard, A., Patriat, M., Basile, C., Loncke, L., Gaullier, V., Folens, L. & Vendeville, B., 2010. Syn- and post-rift evolution of the Demerara Plateau, French Guinea transform margin, *Geophys. Res. Abstr.*, **12**, doi:EGU2010-10979M.
- Mckenzie, D., 1978. Some remarks on the development of sedimentary basins, *Earth planet. Sci. Lett.*, **40**, 25–32.
- Mjelde, R., Raum, T., Myhren, B., Shimamura, H., Murai, Y., Takanami, T., Karpuz, R. & Næss, U., 2005. Continent-ocean transition on the Vøring Plateau, NE Atlantic, derived from densely sampled ocean bottom seismometer data, *J. geophys. Res.*, **110**, B05101, doi:10.1029/2004JB003026.
- Mooney, W.D. & Braille, L.W., 1989. The seismic structure of the continental crust and upper mantle of North America, in *The Geology of North America*, v. A, *The Geology of North America: An overview*, pp. 39–52, eds Bally, A.W. & Palmer, A.R., Geological Society of America, Boulder, CO.
- Nielsen, T.K., Larsen, H.C. & Hopper, J.R., 2002. Contrasting rifted margin styles south of Greenland: implications for mantle plume dynamics, *Earth planet. Sci. Lett.*, **200**, 271–286.
- Nøhr-Hansen, H., 2003. Dinoflagellate cyst stratigraphy of the Palaeogene strata from Hellefisk-1, Ikermiut-1, Kangâmiut-1, Nukik-1, Nukik-2 and Qulleq-1 wells, offshore West Greenland, *Mar. Pet. Geol.*, **20**, 987–1016.
- Nøhr-Hansen, H., Piasecki, S., Rasmussen, J.A. & Sheldon, E., 2000. Biostratigraphy of well 6354/4-1 (Qulleq-1), West Greenland, *Rapp. Danmarks Grønlands Geol. Unders.*, **101**, 81.
- Pegrum, R.M., Ødegård, T., Bonde, K. & Hamann, N.E., 2001. Exploration in the Fylla Area, SW Greenland, in *Proceedings of AAPG Regional Conference*, St. Petersburg, 2001 July 15–18.
- Pinet, B. & Colletta, B., 1990. Probing into extensional sedimentary basins: comparison of recent data and derivation of tentative models, *Tectonophysics*, **173**, 185–197.
- Reston, T., 2005. Polyphase faulting during the development of the west Galicia rifted margin, *Earth planet. Sci. Lett.*, **237**, 561–576.
- Riisager, J., Riisager, P. & Pedersen, A.K., 2003. Paleomagnetism of large igneous provinces: case-study from West Greenland, North Atlantic igneous province, *Earth planet. Sci. Lett.*, **214**, 409–425.
- Roest, W.R. & Srivastava, S.P., 1989a. Sea-floor spreading in the Labrador Sea: a new reconstruction, *Geology*, **17**, 1000–1003.
- Roest, W.R. & Srivastava, S.P., 1989b. Sea floor spreading history in the Labrador Sea. Magnetic anomalies along track. Scale 1:2,000,000, in *East Coast Basin Atlas Series: Labrador Sea*, **86**, ed. J.S. Bell, Geological Survey of Canada, Atlantic Geoscience Centre, Dartmouth, N.S.
- Rolle, F., 1985. Late Cretaceous–Tertiary sediments offshore central West Greenland: lithostratigraphy, sedimentary evolution, and petroleum potential, *Can. J. Earth Sci.*, **22**, 1001–1019.
- Smith, W.H.F. & Sandwell, D.T., 1994. Bathymetric prediction from dense satellite altimetry and sparse shipboard bathymetry, *J. geophys. Res.*, **99**, 21 803–21 824.
- Srivastava, S.P., 1978. Evolution of the Labrador Sea and its bearing on the early evolution of the North Atlantic, *Geophys. J. R. astr. Soc.*, **52**, 313–357.
- Srivastava, S.P. & Roest, W.R., 1995. Nature of thin crust across the south-west Greenland margin and its bearing on the ocean–continent boundary, in *Proceedings of the NATO-ARW workshop on Rifted Ocean–Continent Boundaries*, 11–14 May 1994, pp. 95–120, eds Banda, E., Torne, M. & Talwani, M., Kulwer Academic Publisher, Mallorca, Spain.
- Srivastava, S.P. & Roest, W.R., 1999. Extent of oceanic crust in the Labrador Sea, *Mar. Pet. Geol.*, **16**, 65–84.
- Srivastava, S.P. & Tapscott, C.R., 1986. Plate kinematics of the North Atlantic, in *The Geology of North America*, **M**, eds Vogt, P.R. & Tucholke, B.E., The Western North Atlantic Region, Geological Society of North America, Boulder, CO.
- Storey, M., Duncan, R.A., Pedersen, A.K., Larsen, L.M. & Larsen, H.C., 1998. 40Ar/39Ar geochronology of the West Greenland Tertiary volcanic province, *Earth planet. Sci. Lett.*, **160**, 569–586.
- Sørensen, A.B., 2006. Stratigraphy, structure and petroleum potential of the Lady Franklin and Maniitsoq Basins, offshore southern West Greenland, *Petrol. Geosci.*, **12**, 221–234.
- Tomasso, M., Underhill, J.R., Hodgkinson, R.A., & Young, M.J., 2008. Structural styles and depositional architecture in the Triassic of the Ninian and Alwyn North fields: implications for basin development and prospectivity in the Northern North Sea, *Mar. Pet. Geol.*, **25**(7), 588–605.
- Umpleby, D.C., 1979. Geology of the Labrador Shelf, *Geological Survey of Canada Paper*, 79–13.
- Vogt, P.R., Jung, W.-Y. & Brozena, J., 1998. Arctic margin gravity highs: deeper meaning for sediment depocentres, *Mar. geophys. Res.*, **20**, 459–477.
- Wernicke, B., 1985. Uniform-sense normal simple shear of the continental lithosphere, *Can. J. Earth Sci.*, **22**, 108–125.
- Wilson, P.G., Turner, J.P. & Westbrook, G.K., 2003. Structural architecture of the ocean–continent boundary at an oblique transform margin through

- deep-imaging seismic interpretation and gravity modelling: equatorial Guinea, West Africa, *Tectonophysics*, **374**, 19–40.
- White, N. & McKenzie D., 1988. Formation of the “steer’s head” geometry of sedimentary basins by differential stretching of the crust and mantle, *Geology*, **16**, 250–253.
- Whittaker, R.C., Hamann, N.E. & Pulvertaft, T.C.R., 1997. A new frontier province offshore northwest Greenland: structure, basin development, and petroleum potential of the Melville Bay area, *AAPG Bull.*, **81**(6), 879–998.
- Zervos, F., 1987. A compilation and regional interpretation of the northern North Sea gravity map, *Geol. Soc. Lond. Spec. Publ.*, **28**, 477–493, doi:10.1144/GSL.SP.1987.028.01.30.
- Ziegler, P.A. & Cloetingh, S., 2004. Dynamic processes controlling evolution of rifted basins, *Earth Sci. Rev.*, **64**, 1–50.

## SUPPORTING INFORMATION

Additional Supporting Information may be found in the online version of this article:

**Part I.** Uninterpreted seismic profiles.

**Part II.** Time-to-depth conversion of seismic horizons and 2D gravity modelling along NUGGET Line 1.

Please note: Wiley-Blackwell are not responsible for the content or functionality of any supporting materials supplied by the authors. Any queries (other than missing material) should be directed to the corresponding author for the article.